

## Electronic Supplementary Information:

### Coarse-grained molecular dynamics simulations of $\alpha$ -1,3-glucan

*Daniel J. Beltran-Villegas<sup>1</sup>, Daniel Intriago<sup>1</sup>, Kyle Kim<sup>2</sup>, Natnael Behabtu<sup>2</sup>, J. David Londono<sup>2</sup>, and Arthi Jayaraman<sup>1,3\*</sup>*

1. Dept. of Chemical and Biomolecular Engineering, University of Delaware, Newark DE 19716
2. DuPont Industrial Biosciences, E. I. DuPont De Nemours and Co., Experimental Station, Wilmington, Delaware 19803
3. Dept. of Materials Science and Engineering, University of Delaware, Newark DE, 19716

#### Table of Contents

<b>S.A. Determination of CG bead position within monomers from the atomistic representation</b>	<b>2</b>
<b>S.B. Determination of the L-L'-L'' angle potential parameters from atomistic simulation results</b>	<b>2</b>
<b>S.C. Determination of hydrogen bonding strength stage-wise increase scheme</b>	<b>3</b>
<b>S.D. Additional CG simulation results for unmodified polymer</b>	<b>4</b>
<b>S.E. Additional CG simulation results for randomly substituted polymer</b>	<b>13</b>
<b>S.F. Additional CG simulation results for targeted substitution of DC sites</b>	<b>28</b>

---

\* Corresponding author [arthij@udel.edu](mailto:arthij@udel.edu)

### S.A. Determination of CG bead position within monomers from the atomistic representation

To determine the position of CG beads in a monomer we start by running an atomistic simulation of 7-mer, 10-mer, and 16-mer  $\alpha$ -1,3-glucan, as described in section II.B.1. From the atomistic simulations we calculate the average position of O2 (oxygen in carbon C4), O4, C5, and O3 with respect to the center of mass of the carbon ring (the location of the backbone bead, BB) using the reference frame given by the BB-BB' vector (the vector joining the BB beads between contiguous monomers),  $\mathbf{rv}_1$ , a vector perpendicular to the plane of the carbon ring,  $\mathbf{rv}_2$ , and a third vector perpendicular to  $\mathbf{rv}_1$  and  $\mathbf{rv}_2$ ,  $\mathbf{rv}_3$ . The average relative positions of O2, O4, C5, and O3, in the reference frame given by  $\mathbf{rv}_1$ ,  $\mathbf{rv}_2$ , and  $\mathbf{rv}_3$ , determine the directions of DC2, DC4, DC6, and L, respectively. The size of the backbone bead is taken as the average distance from the center of mass of the carbon ring to the carbons along the ring.

### S.B. Determination of the L-L'-L'' angle potential parameters from atomistic simulation results

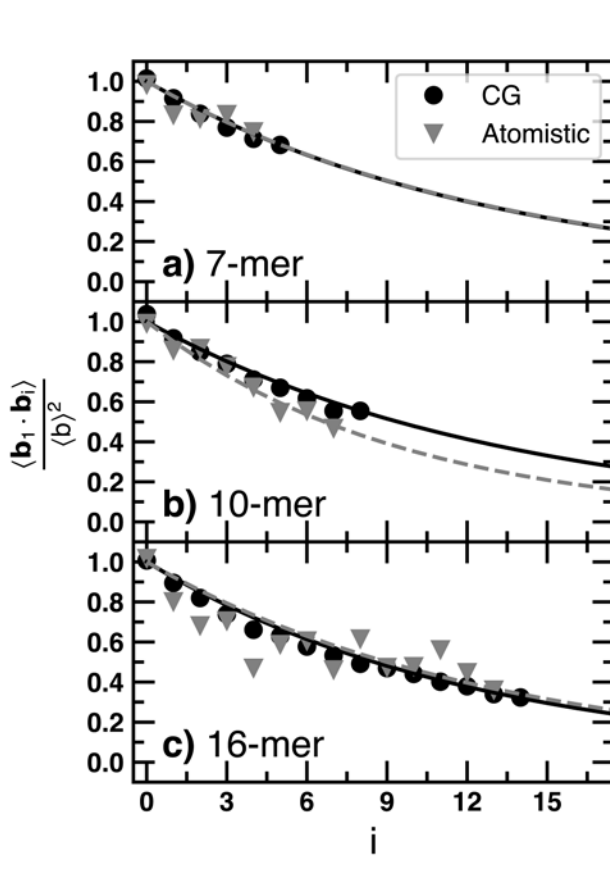


**Figure S1.** Bond correlation as a function of number of repeat unit comparison between atomistic (grey triangles) and coarse-grained (black circles) representations of  $\alpha$ -1,3-glucan for degrees of polymerization DP = 7 (panel a), DP = 10 (panel b), and DP = 16 (panel c).

To determine angle potential parameter  $k_\theta$  we use the atomistic simulation results from section II.B.1 in the main manuscript and calculate the persistence length,  $L_p$ , of 7-mer, 10-mer, and 16-mer chains given by<sup>1</sup>

$$\frac{\langle \mathbf{b}_i \cdot \mathbf{b}_1 \rangle}{\langle b \rangle^2} = \exp\left(-\frac{i}{L_p}\right), \quad (\text{S.1})$$

where  $\mathbf{b}_i$  is the vector joining one end of the chain to segment  $i$  and  $\mathbf{b}_1$  is the vector corresponding to the first chain segment direction. Equation (S.1) presents the bond correlation as a function of the number of segment within a chain.

We vary  $k_0$  in single chain CG simulations to match not only  $L_p$ , but the entire function given by (S.1). In Figure S1 we present the comparison between atomistic and CG simulations for single 7-mer, 10-mer, and 14-mer chains for  $k_0 = 6$  kcal/mol.rad<sup>2</sup>. The resulting persistence length for all chain lengths explored is approximately 13 repeat units (~5 nm).

### S.C. Determination of hydrogen bonding strength stage-wise increase scheme

In this section we present the rationale behind our choice of hydrogen bond strength stage-wise increase scheme. As we mention in the Methods section, we increase  $\epsilon_{AD}$  in a stage-wise fashion to prevent the formation of kinetically trapped structures. To determine the number of timesteps per stage in the scheme we test several annealing schemes ranging from  $1 \times 10^6$  timesteps per stage to  $5 \times 10^6$  timesteps per stage. For each simulation we calculate  $\langle N_{\text{cluster}} \rangle$  as a function of  $\epsilon_{AD}$ , as shown in Figure S2. Our results show that  $\langle N_{\text{cluster}} \rangle$  vs.  $\epsilon_{AD}$  changes dramatically from  $1 \times 10^6$  to  $3 \times 10^6$  timesteps per stage, but not significantly for  $3 \times 10^6$  and above timesteps per stage. We choose  $4 \times 10^6$  timesteps per stage, as increasing the number of timesteps per stage from this particular scheme does not change our results.

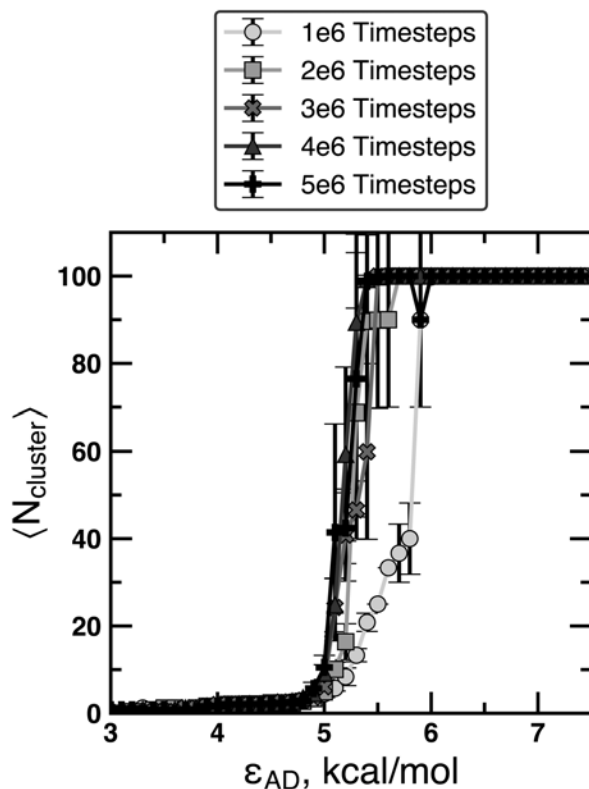


**Figure S2.** Effect of hydrogen bonding strength,  $\epsilon_{AD}$ , and number of timesteps per stage at constant  $\epsilon_{AD}$  for unmodified 5-mer chains on average number of chains per cluster,  $N_{\text{cluster}}$ , of  $\alpha$ -1,3-glucan at  $c_p = 60$  mg/mL. Error bars denote standard deviation over 3 replicas and 250 frames per replica.

### S.D. Additional CG simulation results for unmodified polymer

In this section we present results for average number of chains per cluster ( $\langle N_{\text{cluster}} \rangle$ ), radius of gyration ( $R_g$ ), relative shape anisotropy ( $\kappa^2$ ), hydrogen bonding frequency ( $f_{\text{H-bond}}$ ) pattern, and simulation snapshots for the whole parameter space explored for unmodified  $\alpha$ -1,3-glucan. The values for degree of polymerization ( $DP$ ) are 5-mer, 7-mer, 10-mer, 14-mer, and 20-mer. The polymer concentrations,  $c_p$ , explored are 60.0 mg/mL and 10.0 mg/mL. The hydrogen bonding strength ( $\epsilon_{\text{AD}}$ ) is explored in the range between 3.0 to 7.5 kcal/mol.

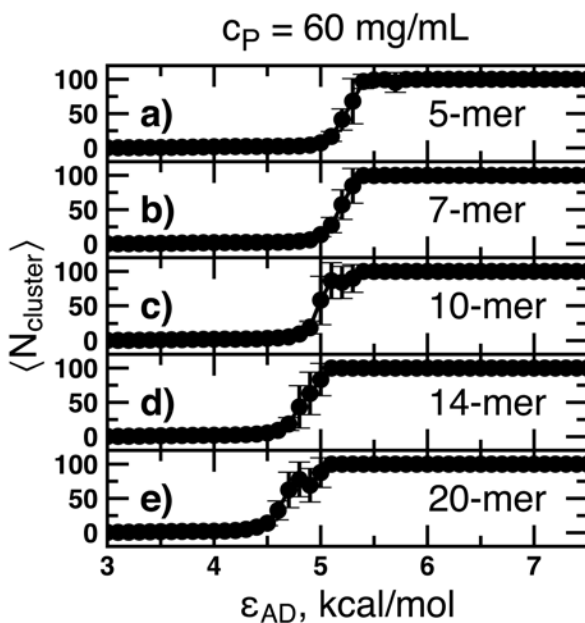


**Figure S3.** Average number of chains per cluster,  $\langle N_{\text{cluster}} \rangle$ , as function of  $\epsilon_{\text{AD}}$  for 5-mer (panel a), 7-mer (panel b), 10-mer (panel c), 14-mer (panel d), and 20-mer (panel e) at a polymer concentration of  $c_p = 60 \text{ mg/mL}$ . Error bars denote standard deviation over 3 replicas and 250 frames per replica.

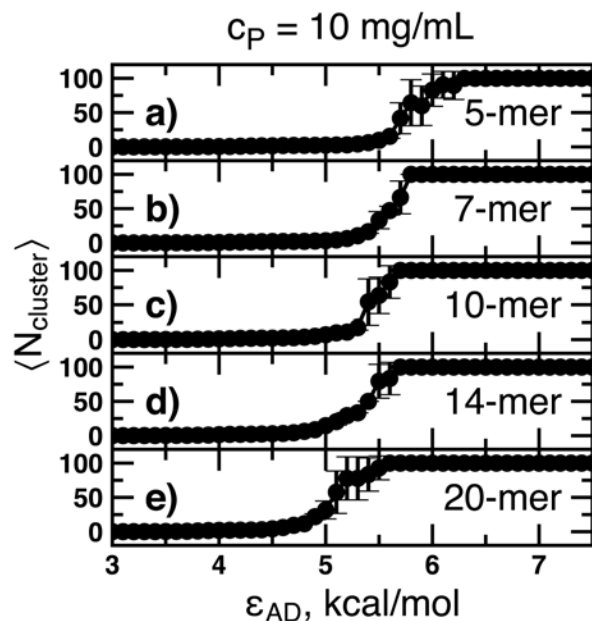


**Figure S4.** Average number of chains per cluster,  $\langle N_{\text{cluster}} \rangle$ , as function of  $\epsilon_{AD}$  for 5-mer (panel a), 7-mer (panel b), 10-mer (panel c), 14-mer (panel d), and 20-mer (panel e) at a polymer concentration of  $c_p = 10 \text{ mg/mL}$ . Error bars denote standard deviation over 3 replicas and 250 frames per replica.

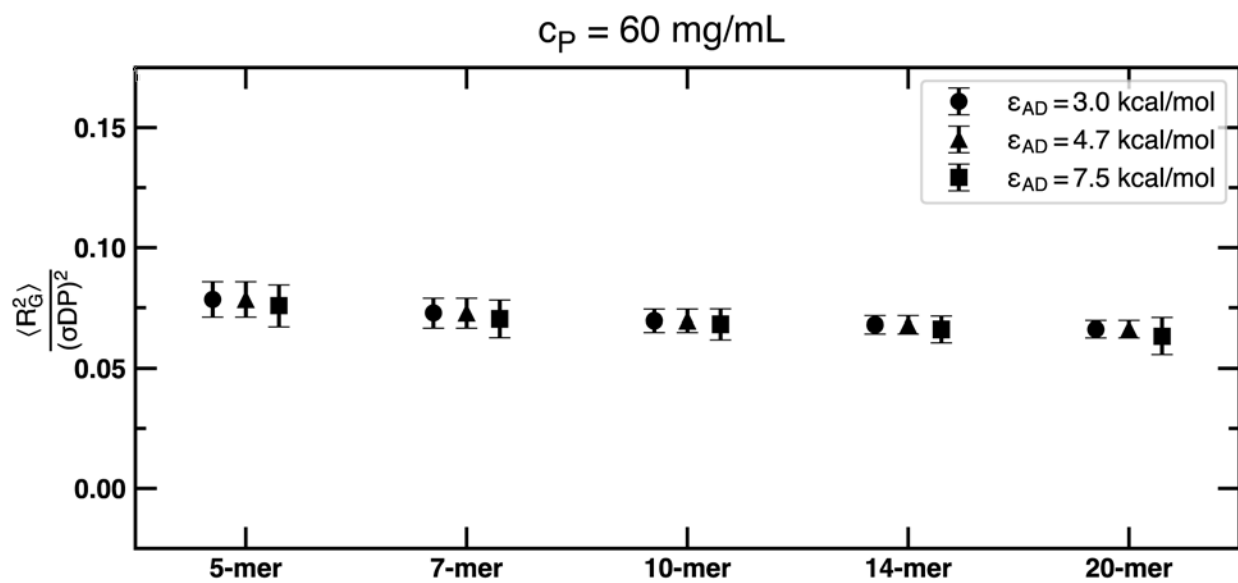


**Figure S5.** Average squared radius of gyration of each chain normalized by contour length ( $\sigma DP$ ) at  $c_p = 60 \text{ mg/mL}$ . Error bars denote standard deviation over 3 replicas and 250 frames per replica.

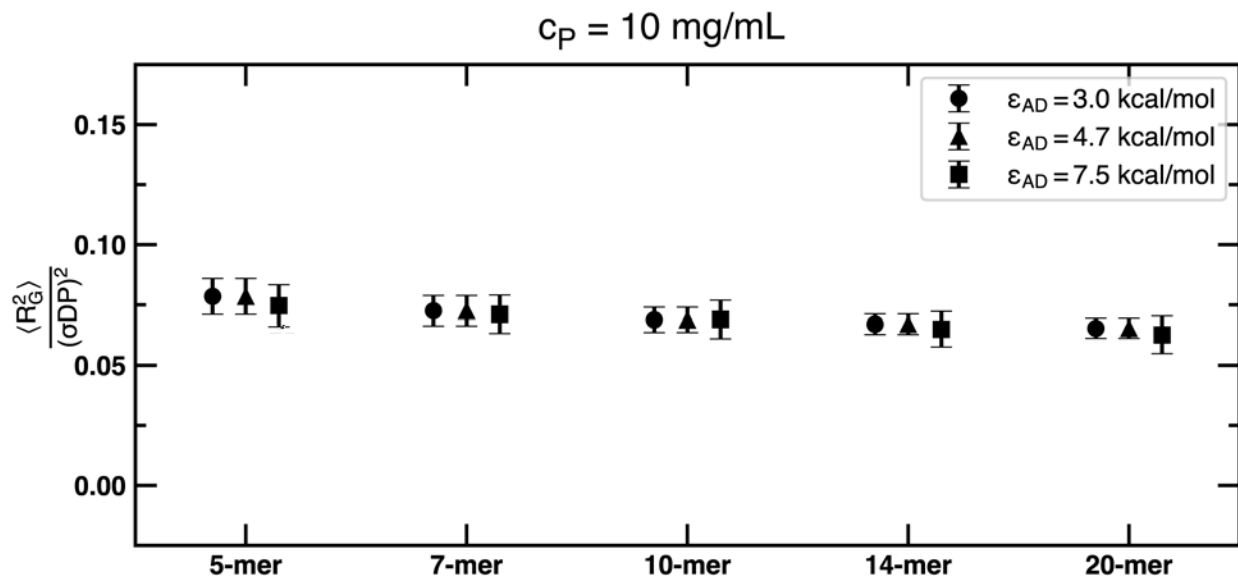


**Figure S6.** Average squared radius of gyration of each chain normalized by contour length ( $\sigma DP$ ) at  $c_p = 10 \text{ mg/mL}$ . Error bars denote standard deviation over 3 replicas and 250 frames per replica.

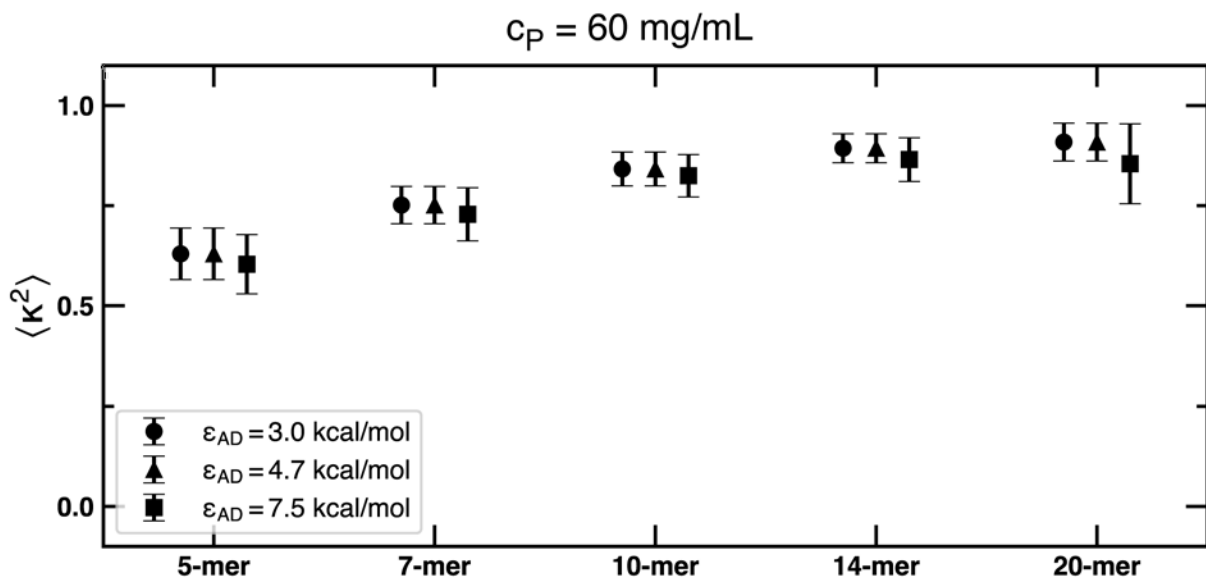


**Figure S7.** Average relative shape anisotropy,  $\kappa^2$ , for each chain at  $c_p = 60 \text{ mg/mL}$ . Error bars denote standard deviation over 3 replicas and 250 frames per replica.

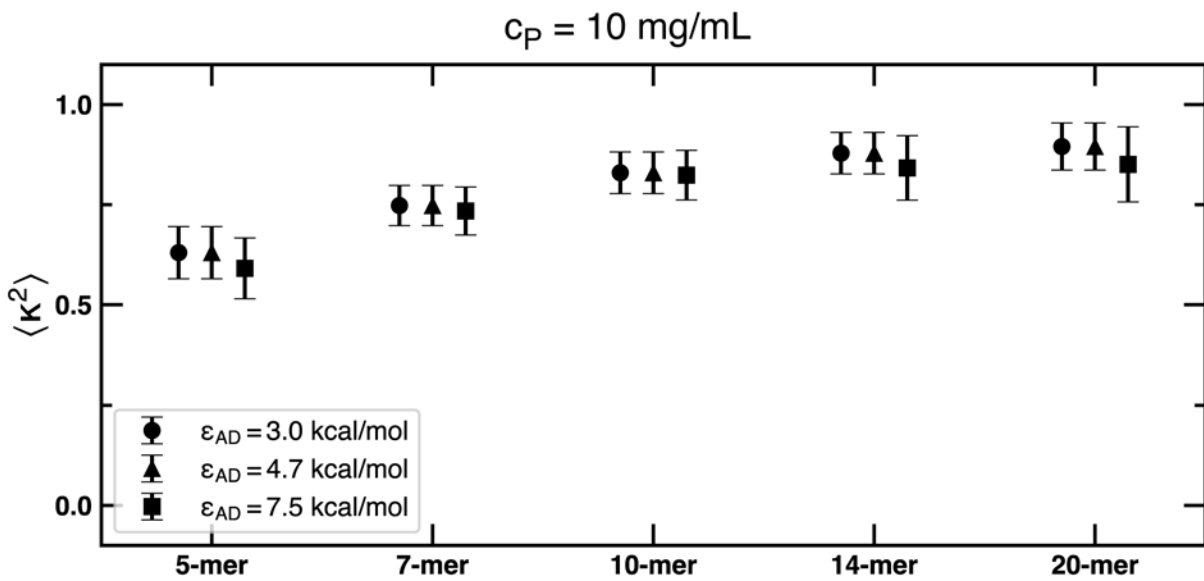


**Figure S8.** Average relative shape anisotropy,  $\kappa^2$ , for each chain at  $c_P = 10 \text{ mg/mL}$ . Error bars denote standard deviation over 3 replicas and 250 frames per replica.

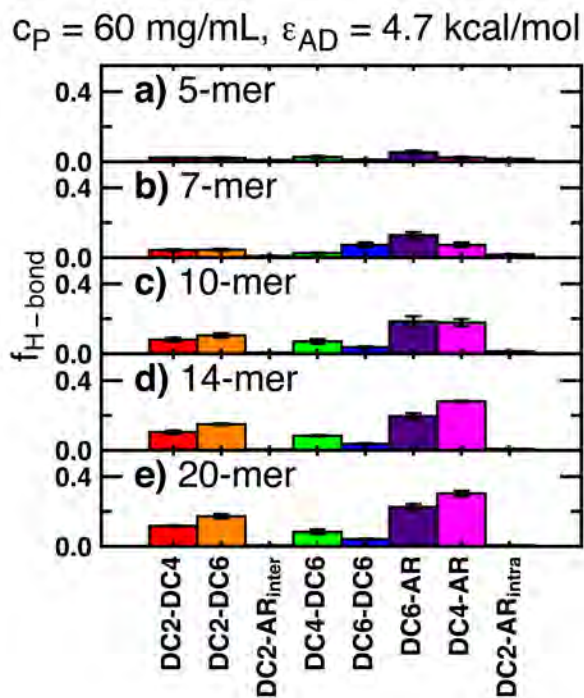


**Figure S9.** Frequency of hydrogen bonds for 5-mer (panel a), 7-mer (panel b), 10-mer (panel c), 14-mer (panel d), and 20-mer (panel e) chains at  $\epsilon_{AD} = 4.7 \text{ kcal/mol}$  at  $c_P = 60 \text{ mg/mL}$ . Error bars are standard deviation of 3 replicas.

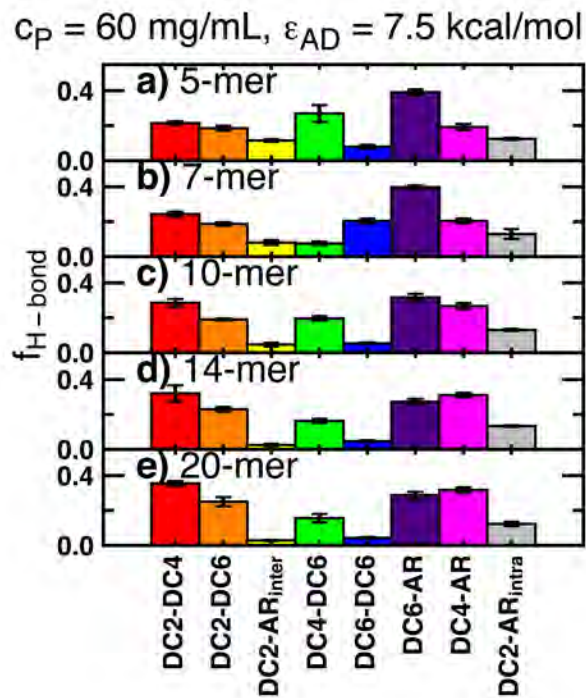


**Figure S10.** Frequency of hydrogen bonds for 5-mer (panel a), 7-mer (panel b), 10-mer (panel c), 14-mer (panel d), and 20-mer (panel e) chains at  $\epsilon_{AD} = 7.5 \text{ kcal/mol}$  at  $c_P = 60 \text{ mg/mL}$ . Error bars are standard deviation of 3 replicas.

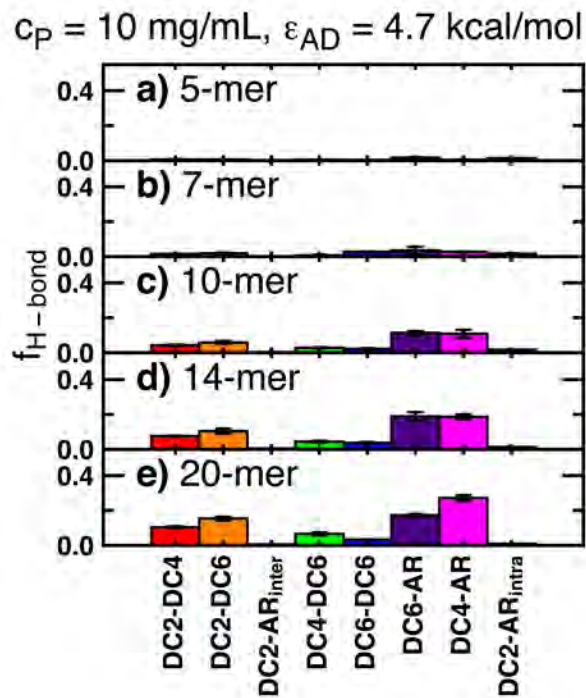


**Figure S11.** Frequency of hydrogen bonds for 5-mer (panel a), 7-mer (panel b), 10-mer (panel c), 14-mer (panel d), and 20-mer (panel e) chains at  $\epsilon_{AD} = 4.7 \text{ kcal/mol}$  at  $c_P = 10 \text{ mg/mL}$ . Error bars are standard deviation of 3 replicas.



$c_P = 10 \text{ mg/mL}$ ,  $\epsilon_{AD} = 7.5 \text{ kcal/mol}$

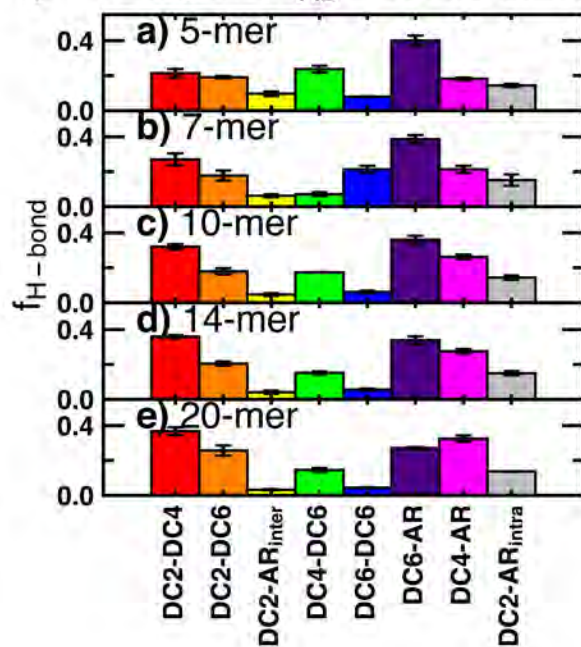


**Figure S12.** Frequency of hydrogen bonds for 5-mer (panel a), 7-mer (panel b), 10-mer (panel c), 14-mer (panel d), and 20-mer (panel e) chains at  $\epsilon_{AD} = 7.5 \text{ kcal/mol}$  at  $c_P = 10 \text{ mg/mL}$ . Error bars are standard deviation of 3 replicas.

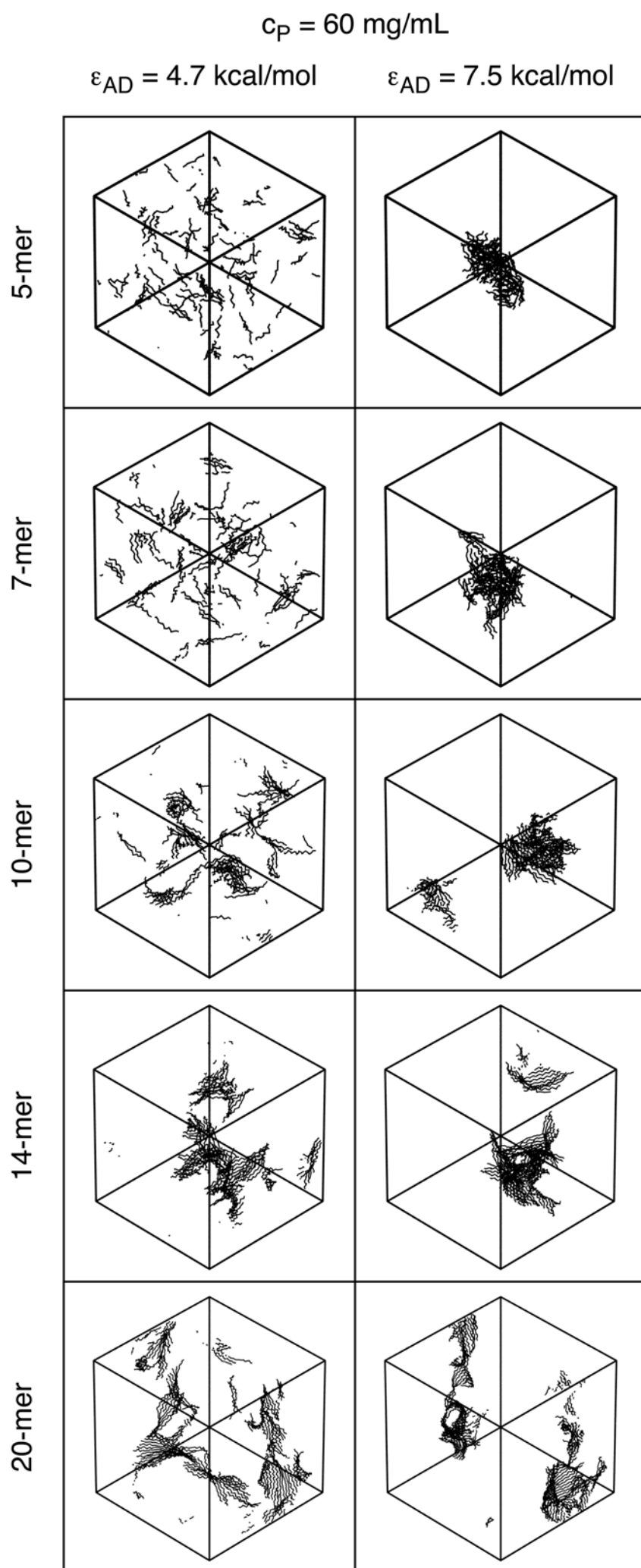


**Figure S13.** Simulation snapshots for unmodified 5-mer, 7-mer, 10-mer, 14-mer, and 20-mer chains at  $\epsilon_{AD} = 4.7$  kcal/mol and 7.5 kcal/mol at  $c_p = 60 \text{ mg/mL}$ .

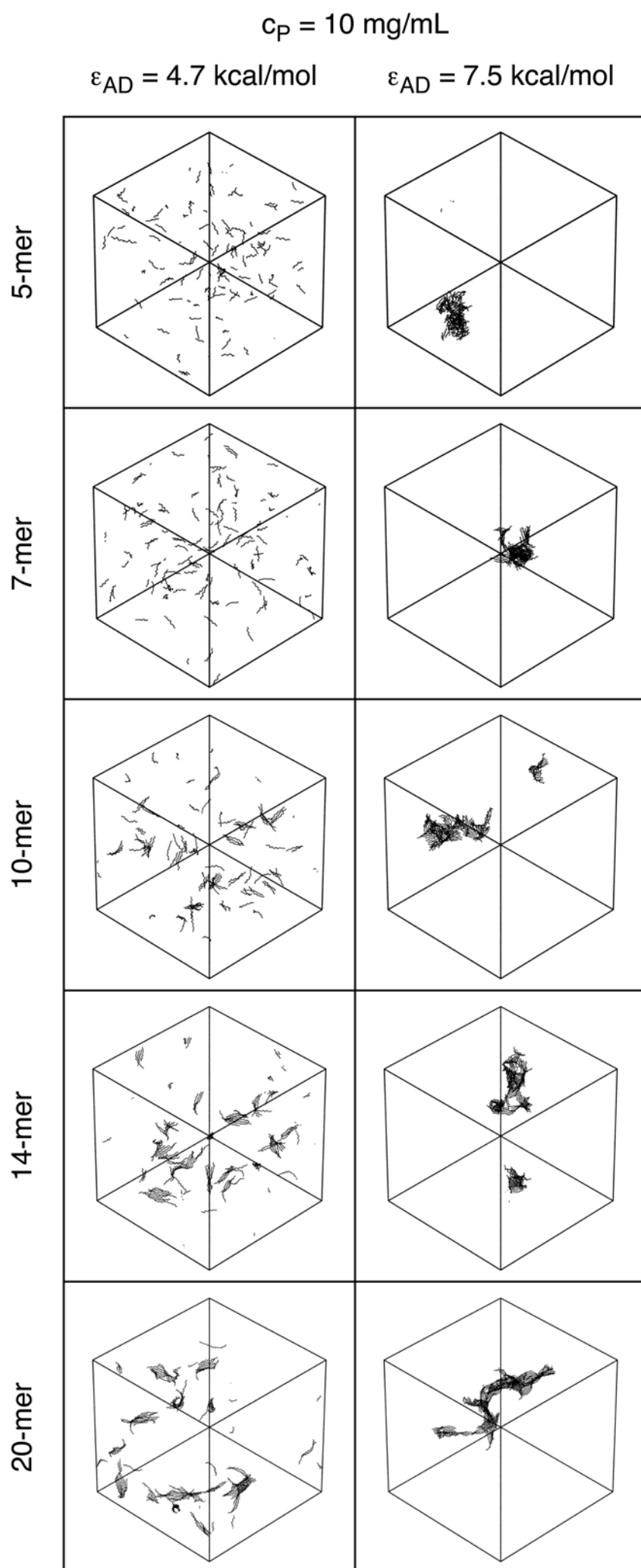


**Figure S14.** Simulation snapshots for unmodified 5-mer, 7-mer, 10-mer, 14-mer, and 20-mer chains at  $\epsilon_{AD} = 4.7$  kcal/mol and 7.5 kcal/mol at  $c_p = 10 \text{ mg/mL}$ .

Figure S15 presents a reproduction of recent microscopy imaging<sup>2</sup> of synthetic  $\alpha$ -1,3-glucan crystal structures formed from precipitation from solution. The images presented below show fibrillar and lamellar structures made of consecutive layers of side-by-side arrangements of  $\alpha$ -1,3-glucan chains, consistent with our findings shown in the Results section and section S.C. for unmodified polymer.

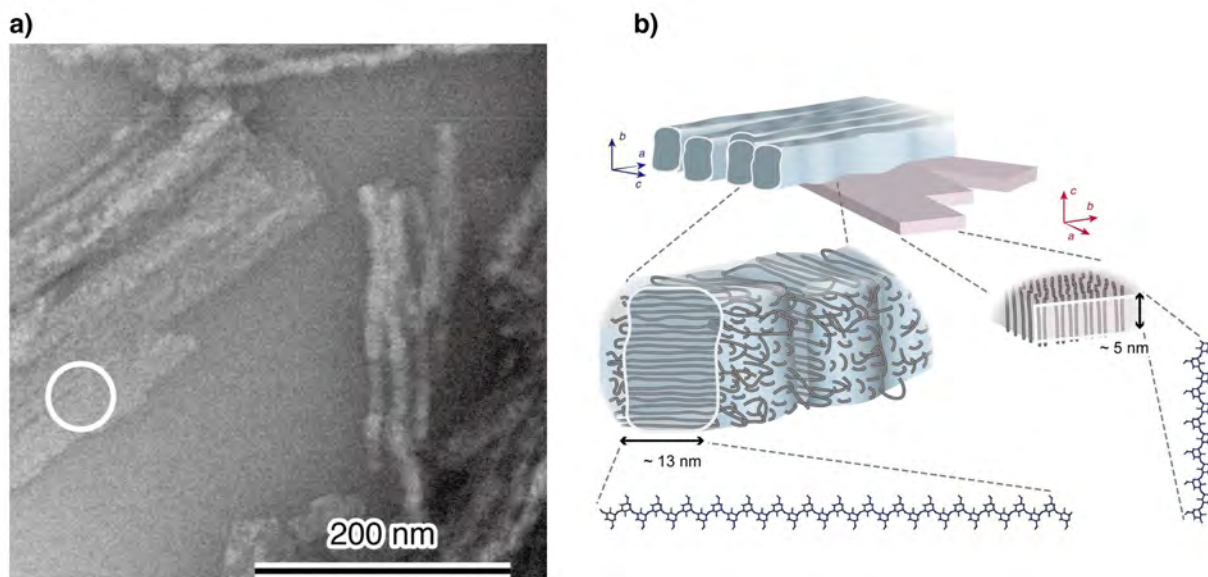


**Figure S15.** Detail of crystal structures from synthesized  $\alpha$ -1,3-glucan assembled from solution. Panel a, TEM image of fibril and lamellar structures. Panel b, schematic representation of chain arrangements in the crystal structure. (Reprinted from Carbohydrate Polymers, 177, K. Kobayashi, T. Hasegawa, R. Kusumi, S. Kimura, M. Yoshida, J. Sugiyama, M. Wada, “Characterization of crystalline linear (1,3)- $\alpha$ -D-glucan synthesized *in vitro*”, 341, 346, Copyright (2017) with permission from Elsevier).

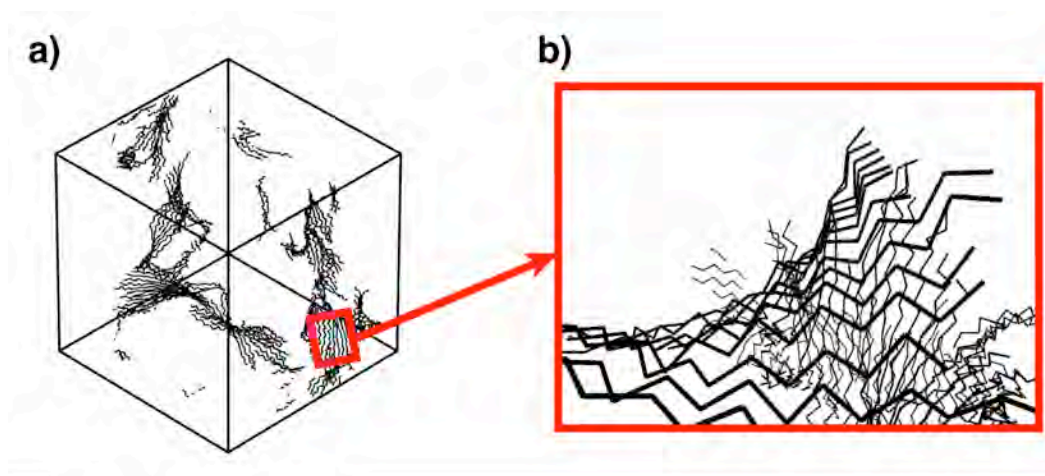


**Figure S16.** Detail of chain stacking for 20-mer chains at  $\epsilon_{AD} = 4.7$  kcal/mol and  $c_P = 60$  mg/mL. a) full simulation box rendering. b) detail of the structure.

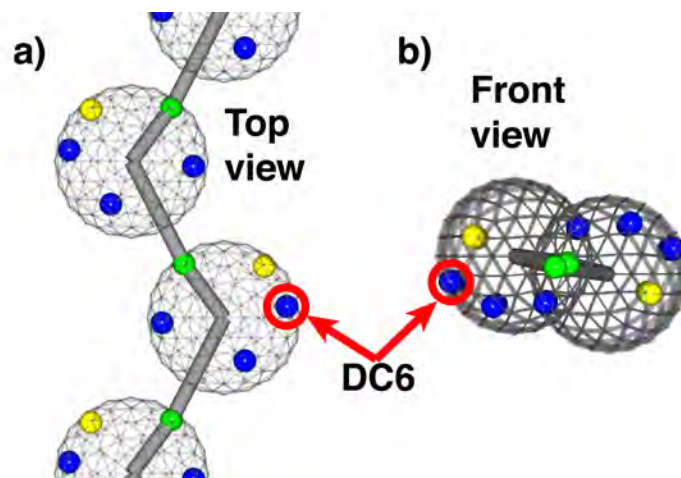


**Figure S17.** Location of the DC6 hydrogen-bonding site in the CG representation of  $\alpha$ -1,3-glucan. a) top view. b) front view.

### S.E. Additional CG simulation results for randomly substituted polymer

In this section we present results for average number of chains per cluster ( $\langle N_{\text{cluster}} \rangle$ ), radius of gyration ( $R_g$ ), relative shape anisotropy ( $\kappa^2$ ), hydrogen bonding frequency ( $f_{\text{H-bond}}$ ) pattern, and simulation snapshots for the whole parameter space explored for  $\alpha$ -1,3-glucan with random substitution of hydrogen bonding sites (DC2, DC4, and DC6). The values for degree of polymerization ( $DP$ ) are 5-mer, 7-mer, 10-mer, 14-mer, and 20-mer. The polymer concentrations,  $c_p$ , explored are 60.0 mg/mL and 10.0 mg/mL. The hydrogen bonding strength ( $\epsilon_{\text{AD}}$ ) is explored in the range between 3.0 to 7.5 kcal/mol. The values for degree of substitution ( $DS$ ) explored are 0.25, 0.50, 0.75, 1.00, 1.25, and 1.50.

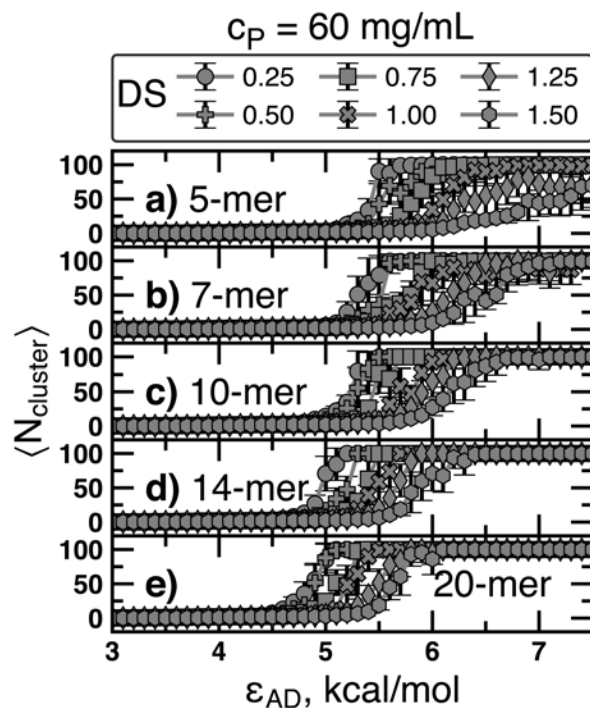


**Figure S18.** Average number of chains per cluster,  $\langle N_{\text{cluster}} \rangle$ , as function of  $\epsilon_{AD}$  for 5-mer (panel a), 7-mer (panel b), 10-mer (panel c), 14-mer (panel d), and 20-mer (panel e) at a polymer concentration of  $c_p = 60 \text{ mg/mL}$  for random substitution of hydrogen bonding sites (DC2, DC4, DC6) at  $DS = 0.25$  (circles),  $DS = 0.50$  (plus symbols),  $DS = 0.75$  (squares),  $DS = 1.00$  (cross symbols),  $DS = 1.25$  (diamonds), and  $DS = 1.50$  (hexagons). Error bars denote standard deviation over 3 replicas and 250 frames per replica.

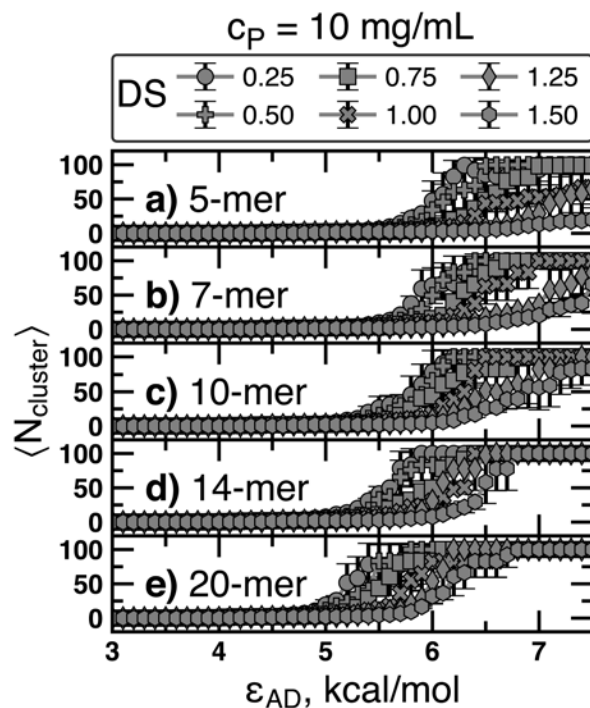


**Figure S19.** Average number of chains per cluster,  $\langle N_{\text{cluster}} \rangle$ , as function of  $\epsilon_{\text{AD}}$  for 5-mer (panel a), 7-mer (panel b), 10-mer (panel c), 14-mer (panel d), and 20-mer (panel e) at a polymer concentration of  $c_p = 10 \text{ mg/mL}$  for random substitution of hydrogen bonding sites (DC2, DC4, DC6) at  $DS = 0.25$  (circles),  $DS = 0.50$  (plus symbols),  $DS = 0.75$  (squares),  $DS = 1.00$  (cross symbols),  $DS = 1.25$  (diamonds), and  $DS = 1.50$  (hexagons). Error bars denote standard deviation over 3 replicas and 250 frames per replica.

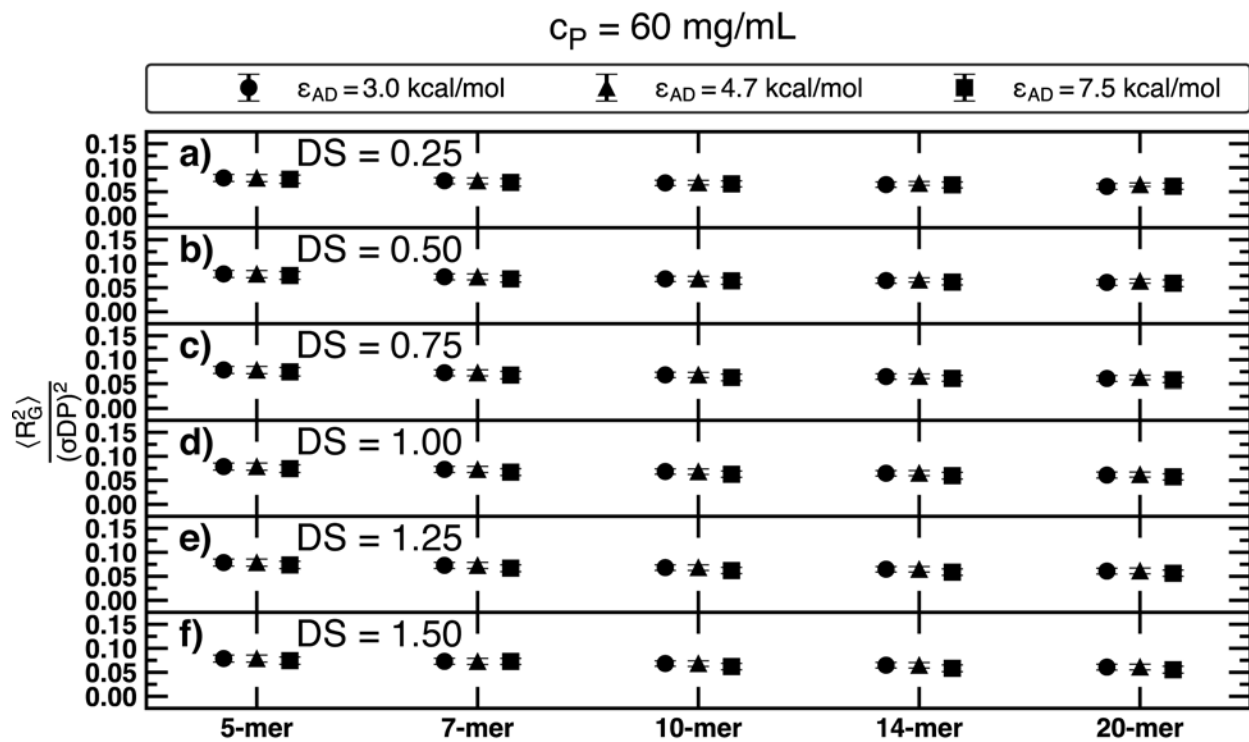


**Figure S20.** Average squared radius of gyration of each chain normalized by contour length ( $\sigma DP$ ) at  $c_p = 60$  mg/mL for degree of substitution  $DS = 0.25$  (panel a),  $DS = 0.50$  (panel b),  $DS = 0.75$  (panel c),  $DS = 1.00$  (panel d),  $DS = 1.25$  (panel e), and  $DS = 1.50$  (panel f). Error bars denote standard deviation over 3 replicas and 250 frames per replica.



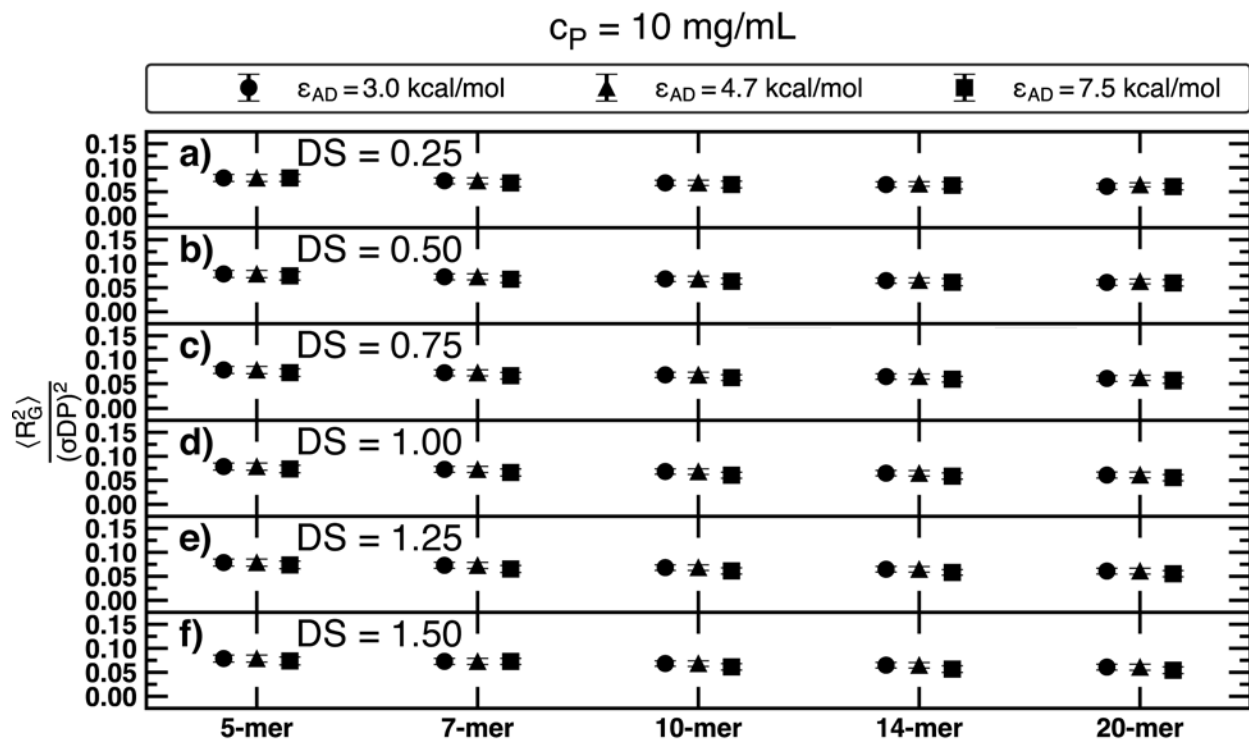


**Figure S21.** Average squared radius of gyration of each chain normalized by contour length ( $\sigma DP$ ) at  $c_p = 10 \text{ mg/mL}$  for degree of substitution  $DS = 0.25$  (panel a),  $DS = 0.50$  (panel b),  $DS = 0.75$  (panel c),  $DS = 1.00$  (panel d),  $DS = 1.25$  (panel e), and  $DS = 1.50$  (panel f). Error bars denote standard deviation over 3 replicas and 250 frames per replica.

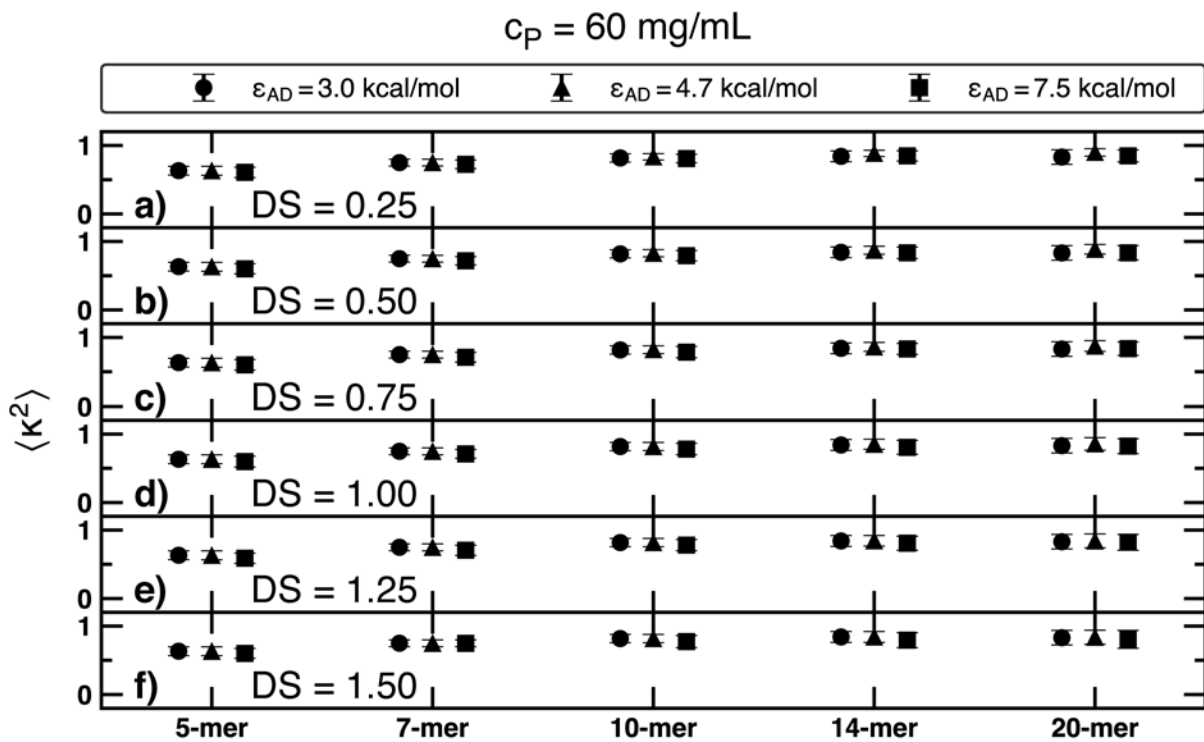


**Figure S22.** Average relative shape anisotropy,  $\kappa^2$ , for each chain at  $c_p = 60 \text{ mg/mL}$  for degree of substitution  $DS = 0.25$  (panel a),  $DS = 0.50$  (panel b),  $DS = 0.75$  (panel c),  $DS = 1.00$  (panel d),  $DS = 1.25$  (panel e), and  $DS = 1.50$  (panel f). Error bars denote standard deviation over 3 replicas and 250 frames per replica.

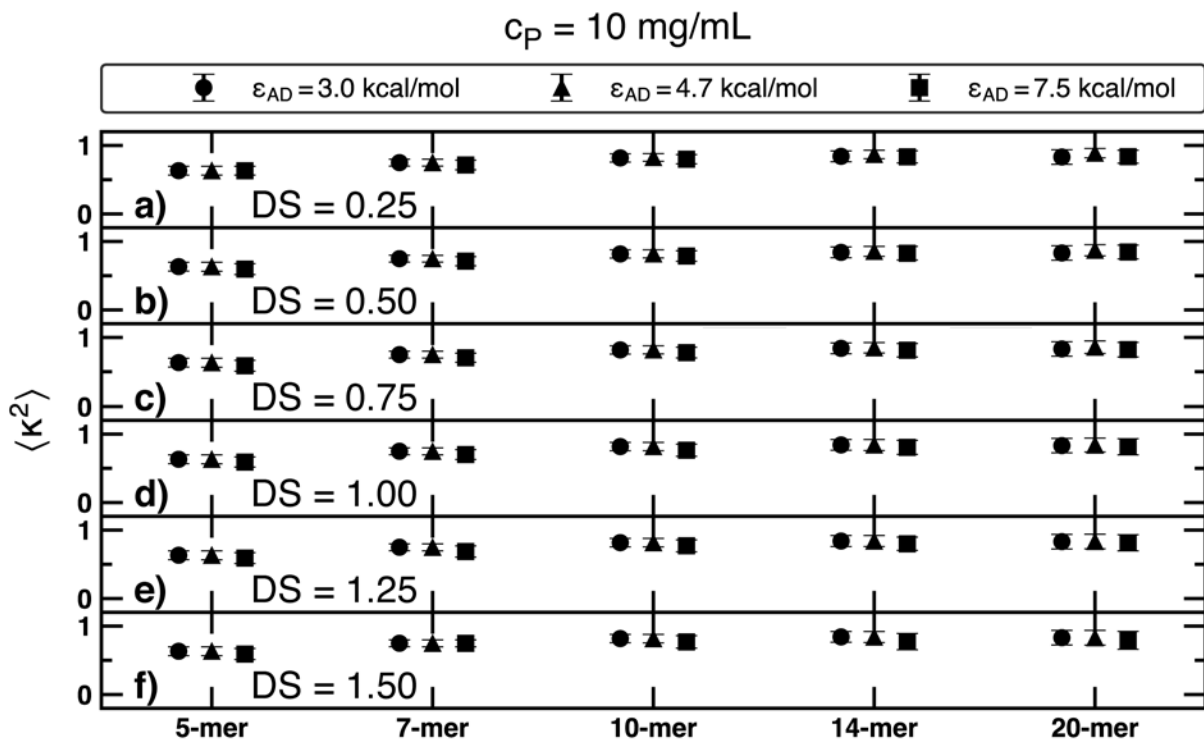


**Figure S23.** Average relative shape anisotropy,  $\kappa^2$ , for each chain at  $c_p = 10 \text{ mg/mL}$  for degree of substitution  $DS = 0.25$  (panel a),  $DS = 0.50$  (panel b),  $DS = 0.75$  (panel c),  $DS = 1.00$  (panel d),  $DS = 1.25$  (panel e), and  $DS = 1.50$  (panel f). Error bars denote standard deviation over 3 replicas and 250 frames per replica.

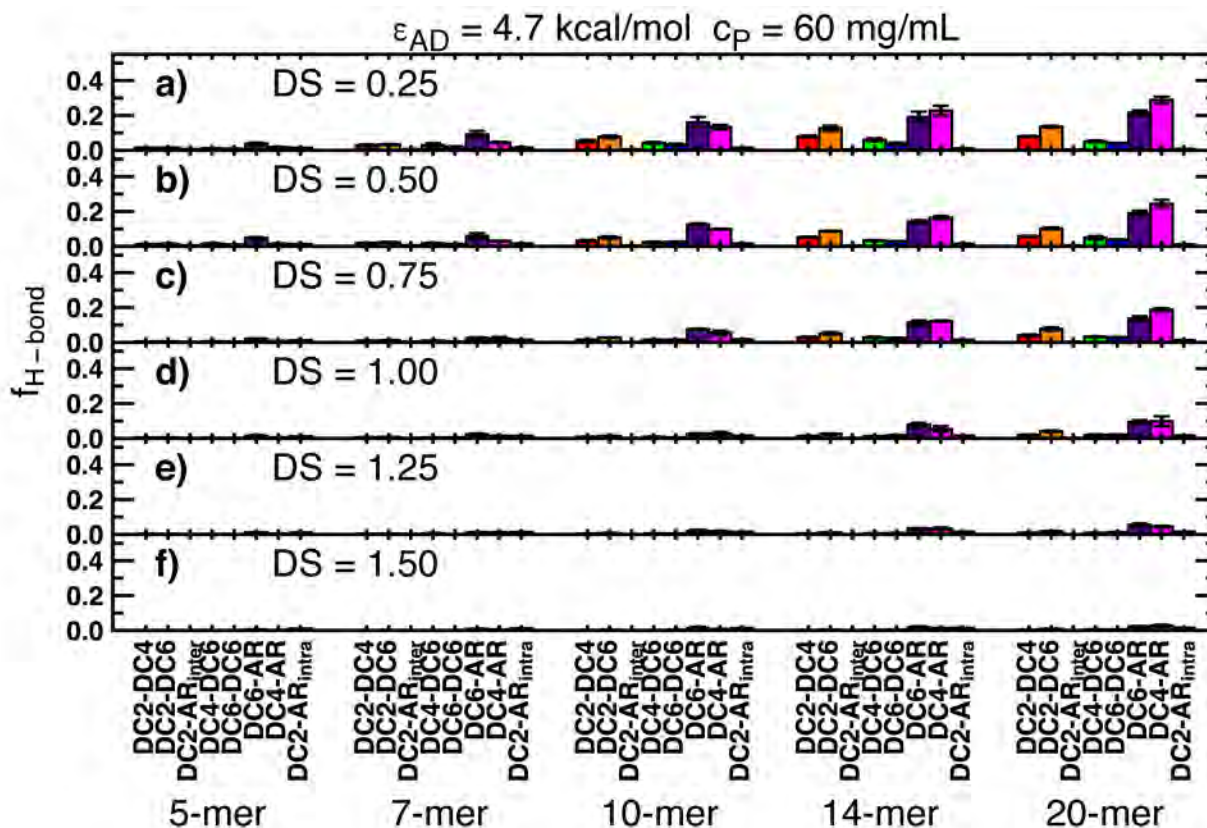


**Figure S24.** Frequency of hydrogen bonds at  $\epsilon_{AD} = 4.7 \text{ kcal/mol}$  and  $c_P = 60 \text{ mg/mL}$  for degree of substitution  $DS = 0.25$  (panel a),  $DS = 0.50$  (panel b),  $DS = 0.75$  (panel c),  $DS = 1.00$  (panel d),  $DS = 1.25$  (panel e), and  $DS = 1.50$  (panel f). Error bars denote standard deviation over 3 replicas.

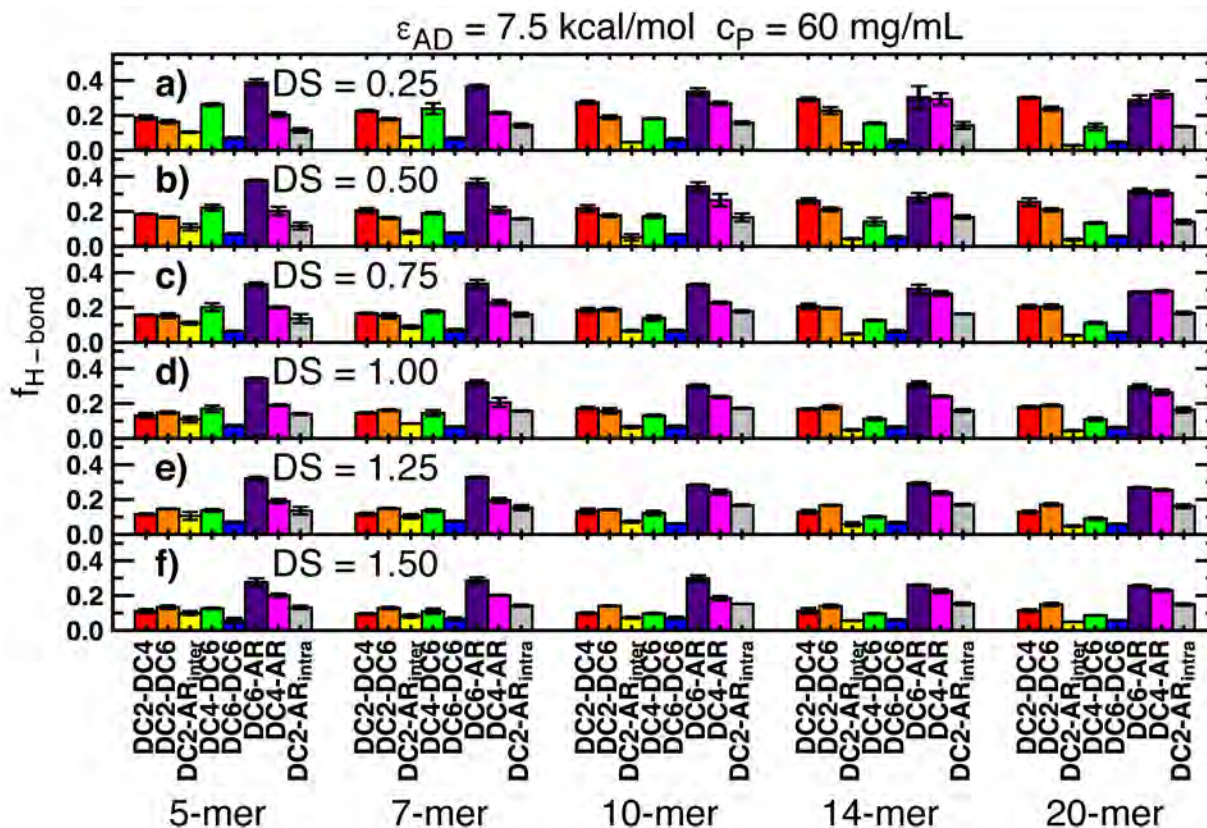


**Figure S25.** Frequency of hydrogen bonds at  $\epsilon_{AD} = 7.5 \text{ kcal/mol}$  and  $c_p = 60 \text{ mg/mL}$  for degree of substitution  $DS = 0.25$  (panel a),  $DS = 0.50$  (panel b),  $DS = 0.75$  (panel c),  $DS = 1.00$  (panel d),  $DS = 1.25$  (panel e), and  $DS = 1.50$  (panel f). Error bars denote standard deviation over 3 replicas.

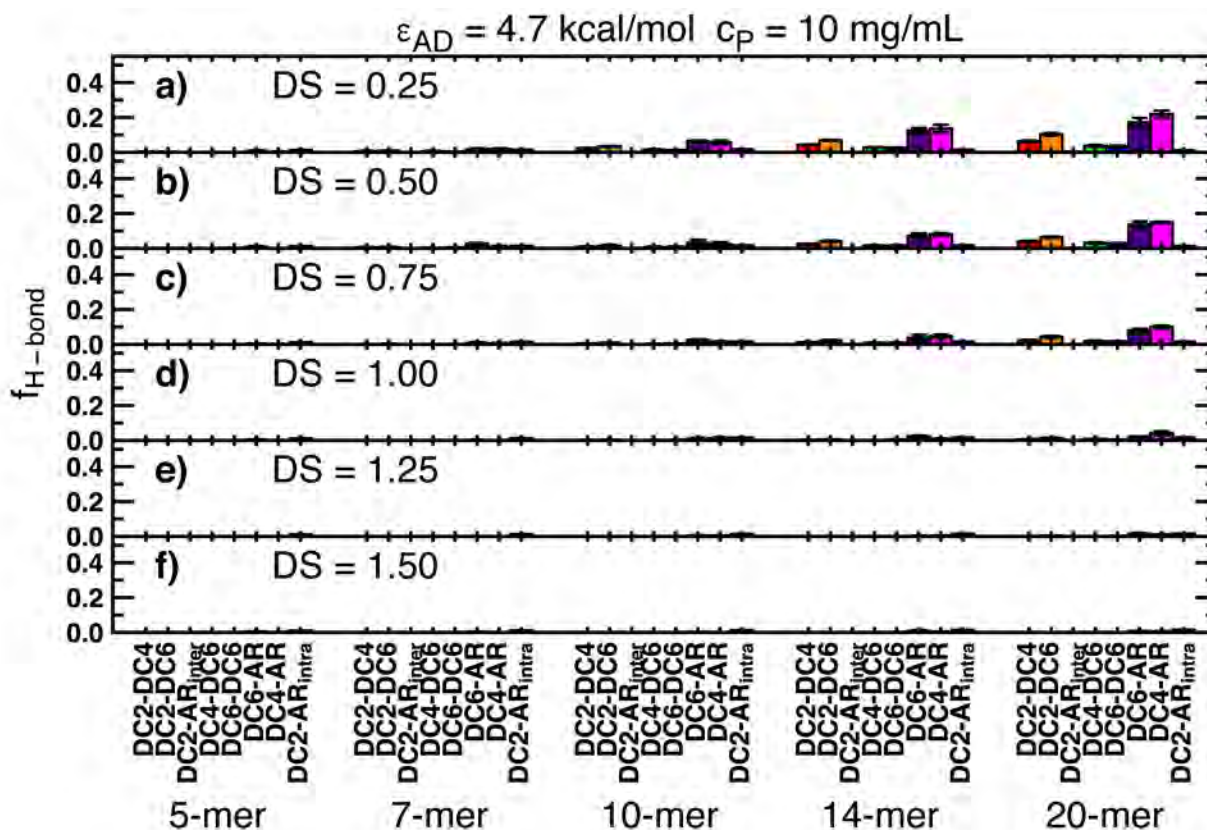


**Figure S26.** Frequency of hydrogen bonds at  $\epsilon_{AD} = 4.7 \text{ kcal/mol}$  and  $c_P = 10 \text{ mg/mL}$  for degree of substitution  $DS = 0.25$  (panel a),  $DS = 0.50$  (panel b),  $DS = 0.75$  (panel c),  $DS = 1.00$  (panel d),  $DS = 1.25$  (panel e), and  $DS = 1.50$  (panel f). Error bars denote standard deviation over 3 replicas.

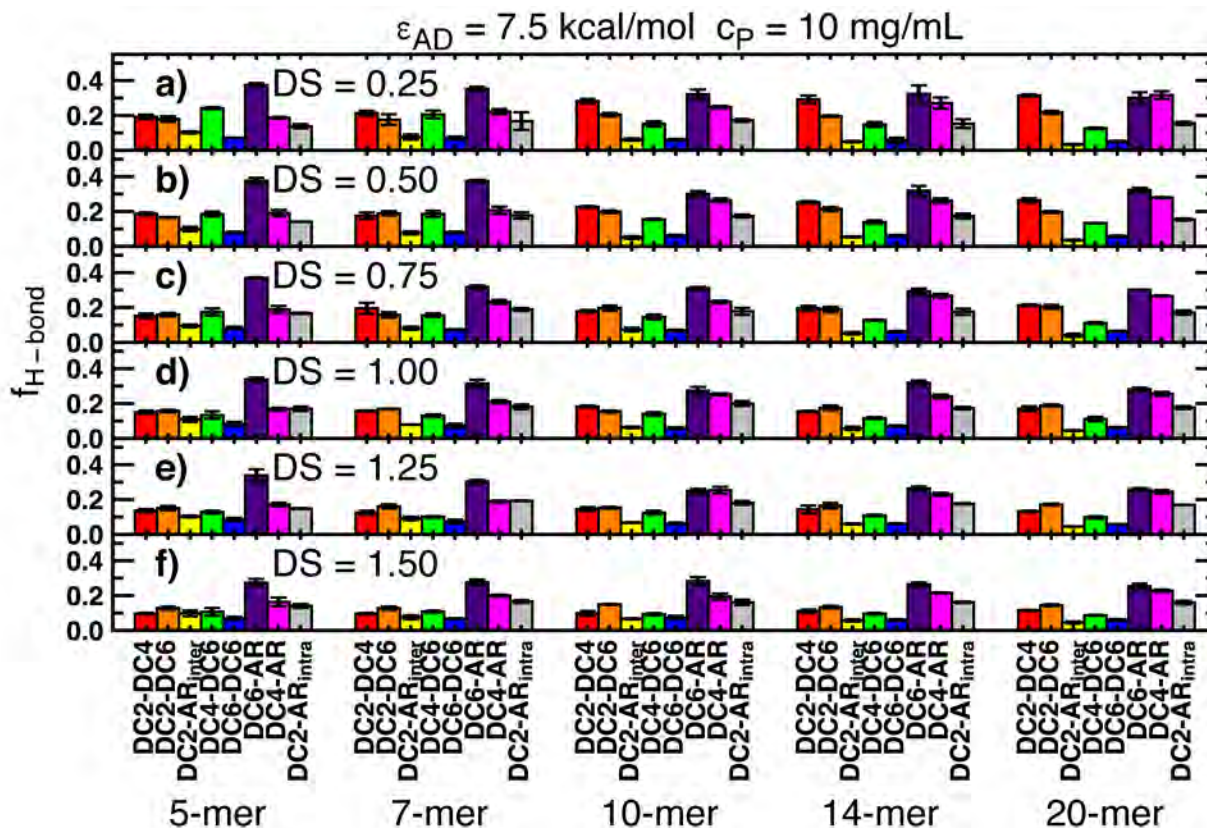


**Figure S27.** Frequency of hydrogen bonds at  $\epsilon_{AD} = 7.5 \text{ kcal/mol}$  and  $c_p = 10 \text{ mg/mL}$  for degree of substitution  $DS = 0.25$  (panel a),  $DS = 0.50$  (panel b),  $DS = 0.75$  (panel c),  $DS = 1.00$  (panel d),  $DS = 1.25$  (panel e), and  $DS = 1.50$  (panel f). Error bars denote standard deviation over 3 replicas.

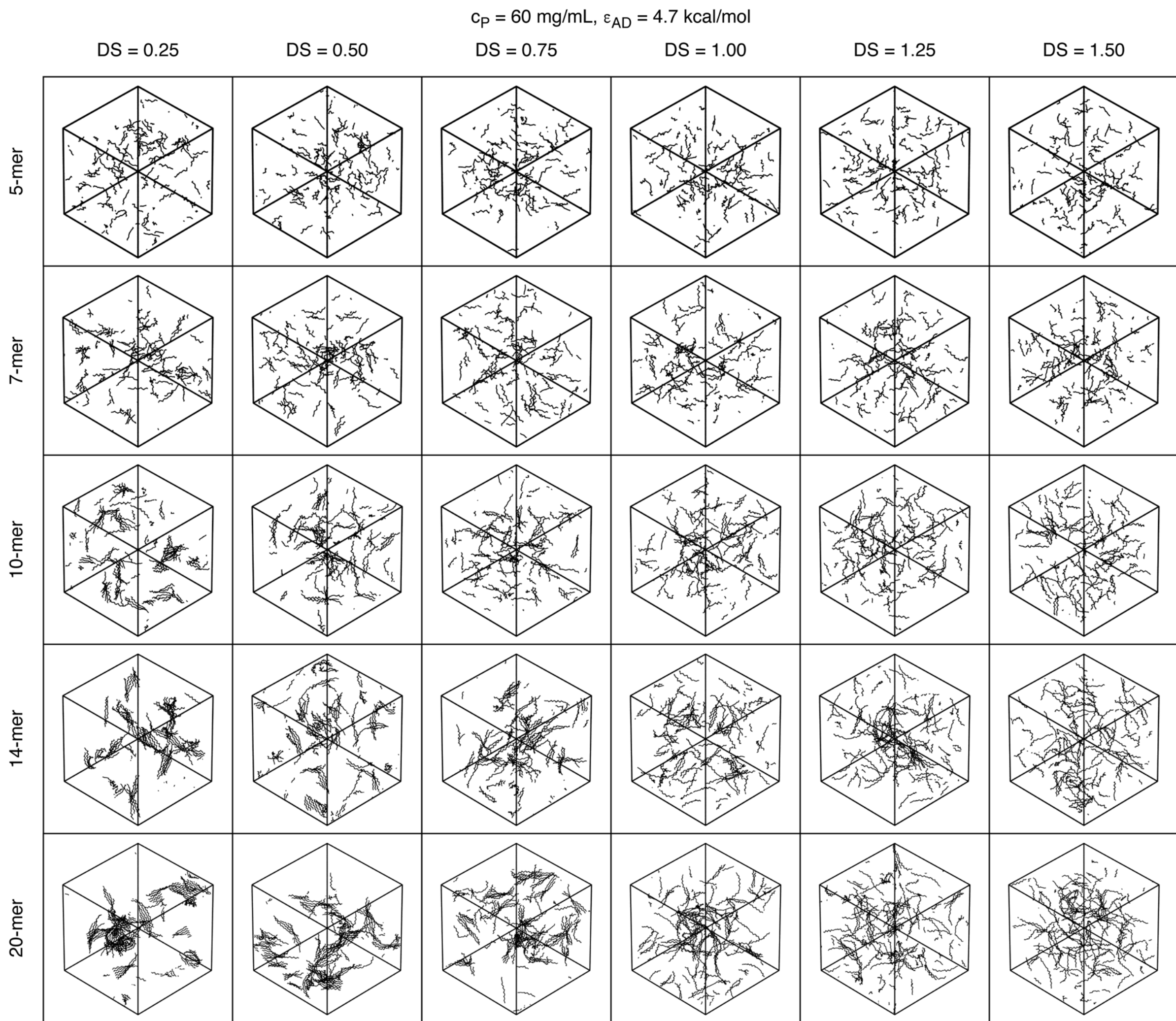


**Figure S28.** Simulation snapshots for randomly substituted 5-mer, 7-mer, 10-mer, 14-mer, and 20-mer chains at  $\epsilon_{AD} = 4.7 \text{ kcal/mol}$  at  $c_p = 60 \text{ mg/mL}$ .



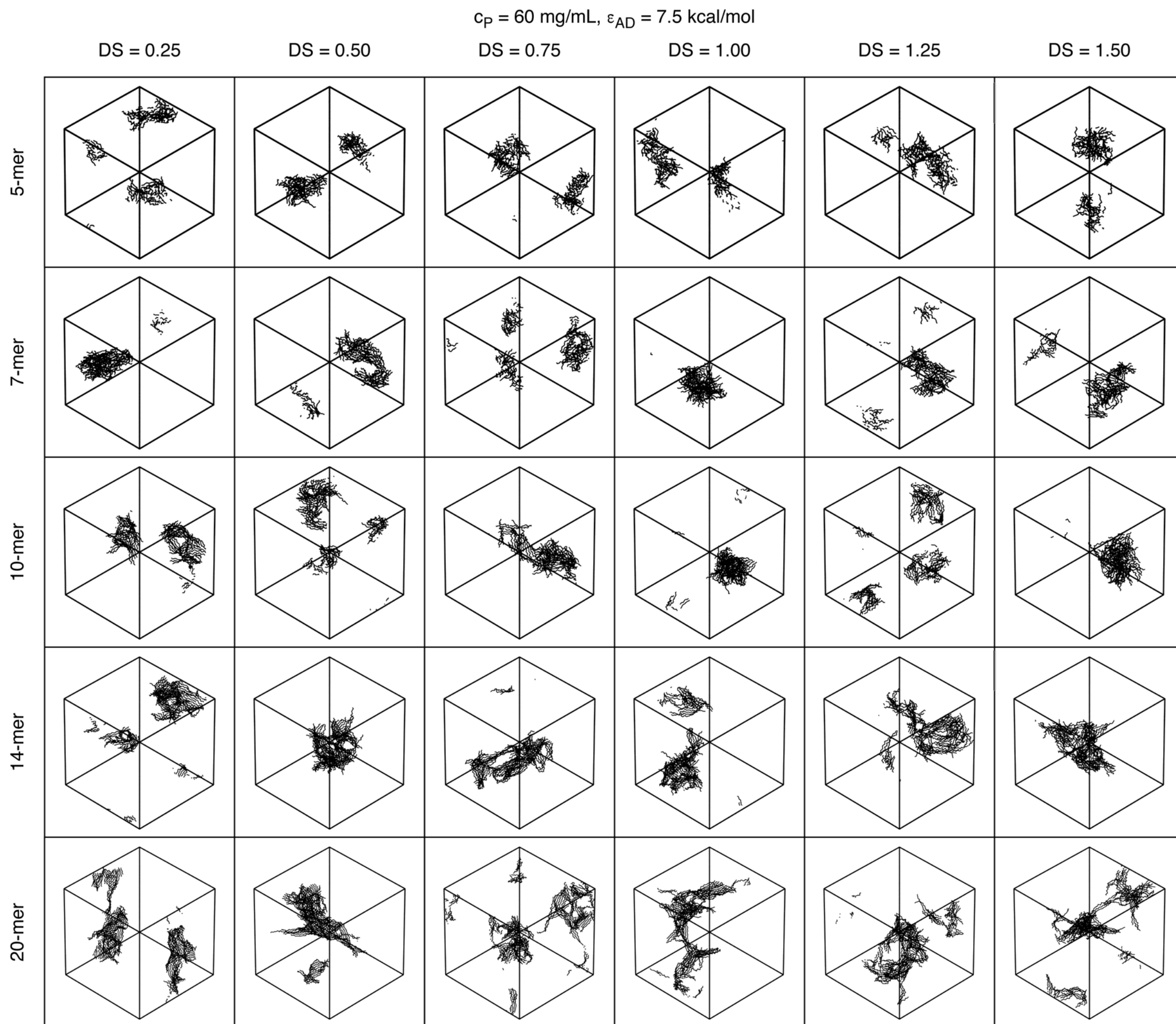


**Figure S29.** Simulation snapshots for randomly substituted 5-mer, 7-mer, 10-mer, 14-mer, and 20-mer chains at  $\epsilon_{AD} = 7.5 \text{ kcal/mol}$  at  $c_p = 60 \text{ mg/mL}$ .

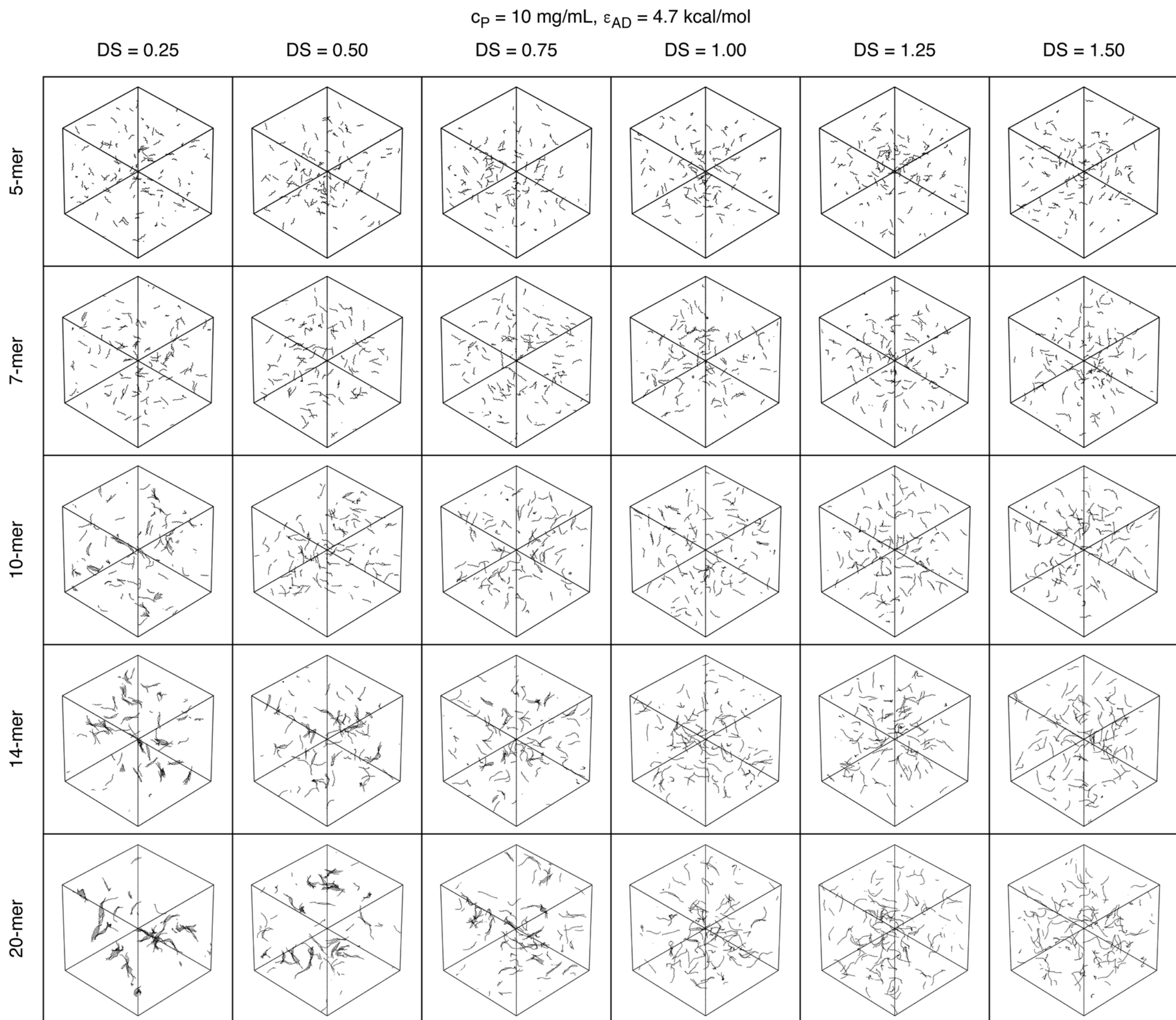


**Figure S30.** Simulation snapshots for randomly substituted 5-mer, 7-mer, 10-mer, 14-mer, and 20-mer chains at  $\epsilon_{AD} = 4.7 \text{ kcal/mol}$  at  $c_p = 10 \text{ mg/mL}$ .

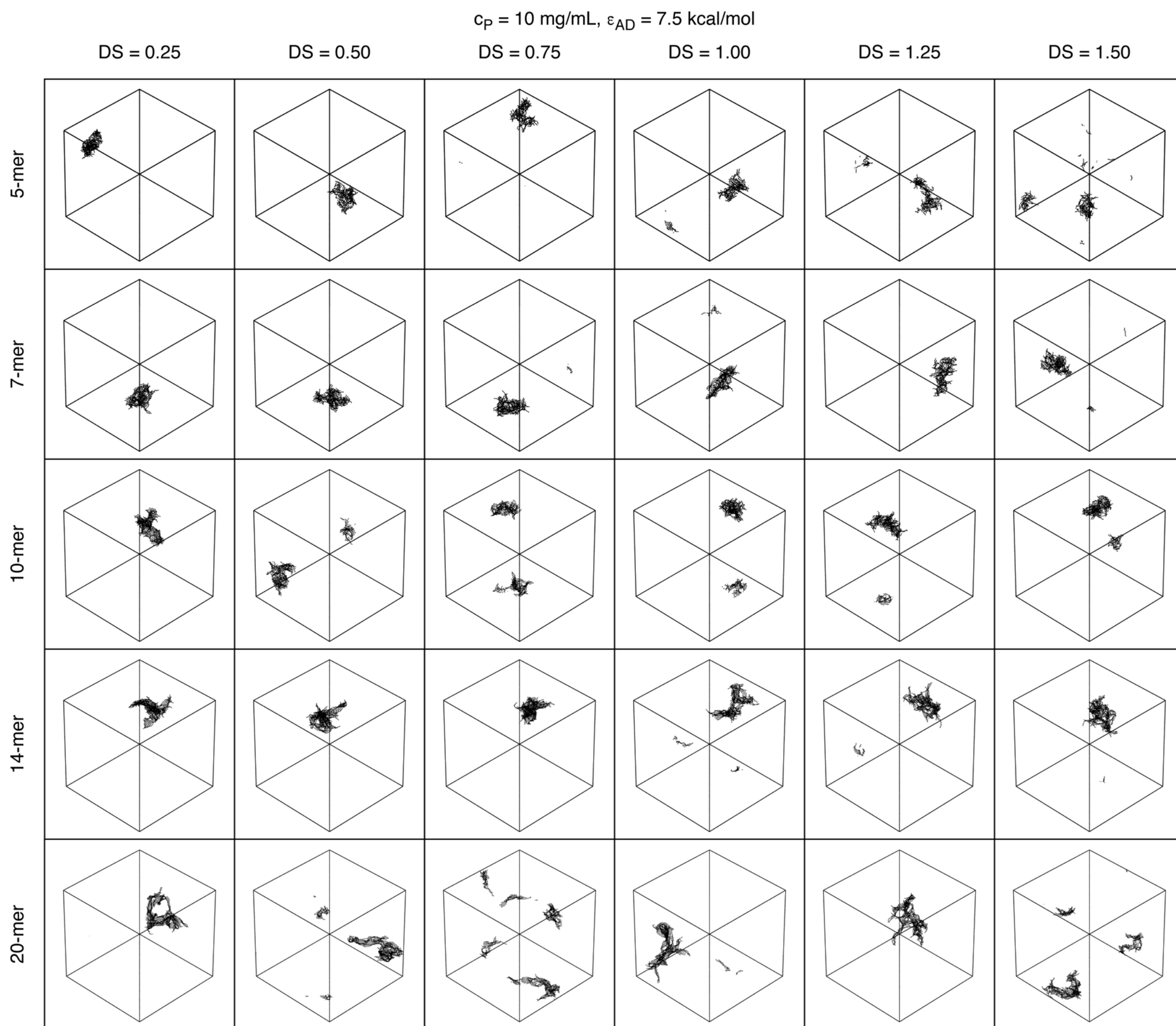


**Figure S31.** Simulation snapshots for randomly substituted 5-mer, 7-mer, 10-mer, 14-mer, and 20-mer chains at  $\epsilon_{AD} = 7.5 \text{ kcal/mol}$  at  $c_p = 10 \text{ mg/mL}$ .

### S.E. Additional CG simulation results for targeted substitution of DC sites

In this section we present results for average number of chains per cluster ( $\langle N_{\text{cluster}} \rangle$ ), radius of gyration ( $R_g$ ), relative shape anisotropy ( $\kappa^2$ ), hydrogen bonding frequency ( $f_{\text{H-bond}}$ ) pattern, and simulation snapshots for the whole parameter space explored for  $\alpha$ -1,3-glucan with targeted substitution of hydrogen bonding sites (DC2, DC4, and DC6). The values for degree of polymerization ( $DP$ ) are 5-mer, 7-mer, 10-mer, 14-mer, and 20-mer. The polymer concentrations,  $c_p$ , explored are 60.0 mg/mL and 10.0 mg/mL. The hydrogen bonding strength ( $\epsilon_{\text{AD}}$ ) is explored in the range between 3.0 to 7.5 kcal/mol.

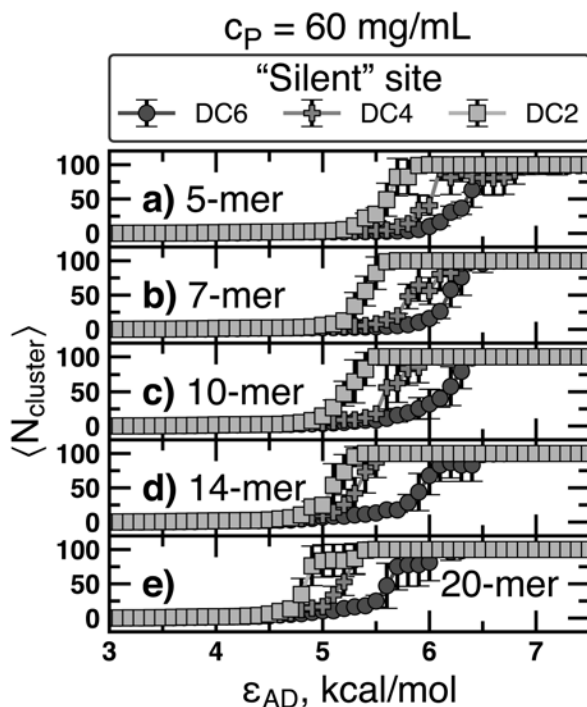


**Figure S32.** Average number of chains per cluster,  $\langle N_{\text{cluster}} \rangle$ , as function of  $\epsilon_{\text{AD}}$  for 5-mer (panel a), 7-mer (panel b), 10-mer (panel c), 14-mer (panel d), and 20-mer (panel e) at a polymer concentration of  $c_p = 60 \text{ mg/mL}$  for targeted substitution of hydrogen bonding sites: DC6 (circles), DC4 (plus symbols), and DC2 (squares). Error bars denote standard deviation over 3 replicas and 250 frames per replica.

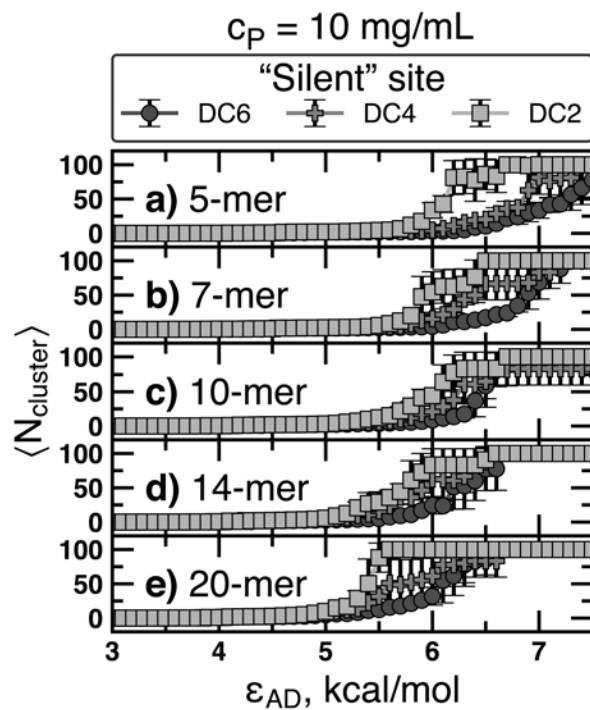


**Figure S33.** Average number of chains per cluster,  $\langle N_{\text{cluster}} \rangle$ , as function of  $\epsilon_{\text{AD}}$  for 5-mer (panel a), 7-mer (panel b), 10-mer (panel c), 14-mer (panel d), and 20-mer (panel e) at a polymer concentration of  $c_p = 10 \text{ mg/mL}$  for targeted substitution of hydrogen bonding sites: DC6 (circles), DC4 (plus symbols), and DC2 (squares). Error bars denote standard deviation over 3 replicas and 250 frames per replica.

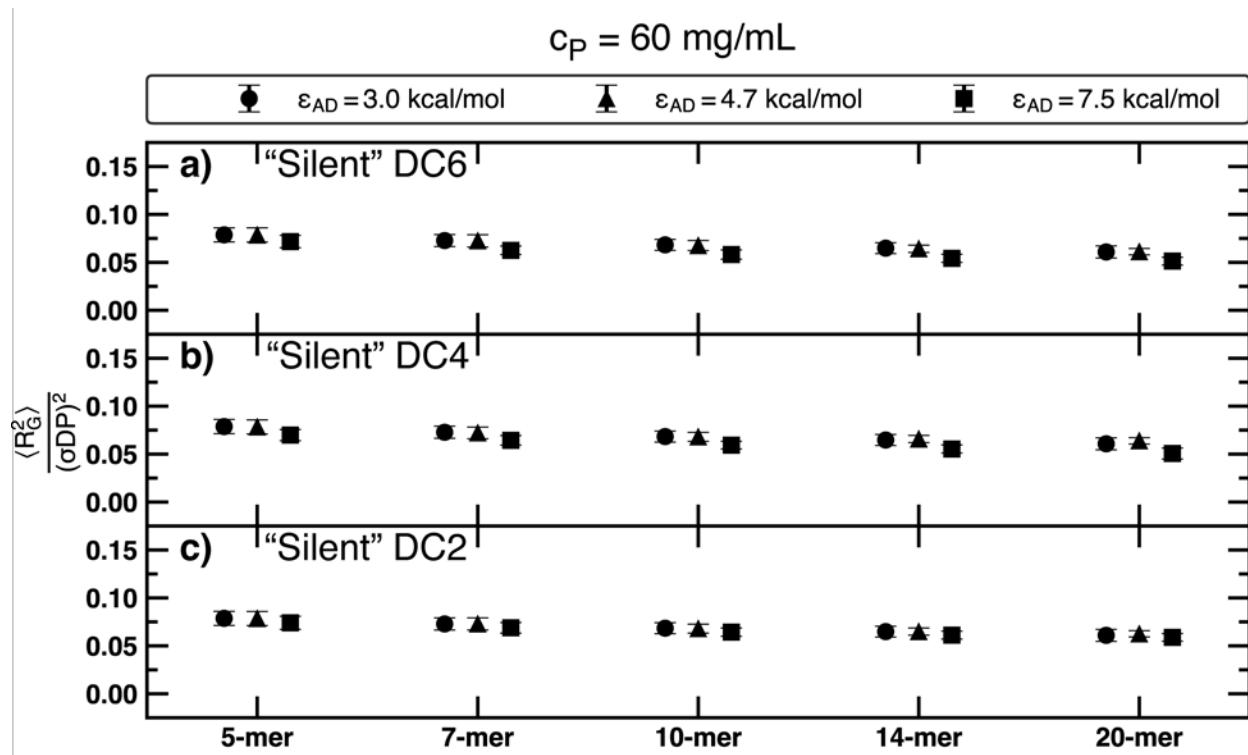


**Figure S34.** Average squared radius of gyration of each chain normalized by contour length ( $\sigma DP$ ) at  $c_p = 60 \text{ mg/mL}$  for targeted substitution of DC6 (panel a), DC4 (panel b), and DC2 (panel c). Error bars denote standard deviation over 3 replicas and 250 frames per replica.

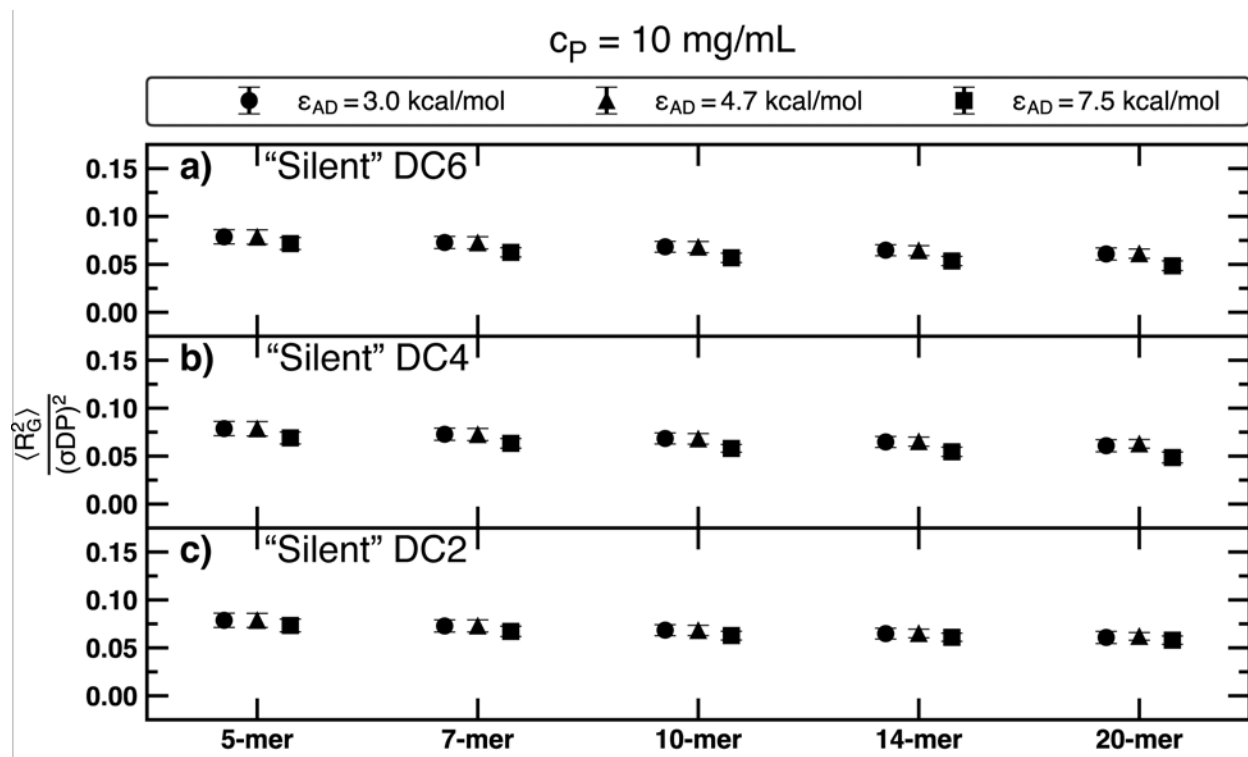


**Figure S35.** Average squared radius of gyration of each chain normalized by contour length ( $\sigma DP$ ) at  $c_p = 10 \text{ mg/mL}$  for targeted substitution of DC6 (panel a), DC4 (panel b), and DC2 (panel c). Error bars denote standard deviation over 3 replicas and 250 frames per replica.

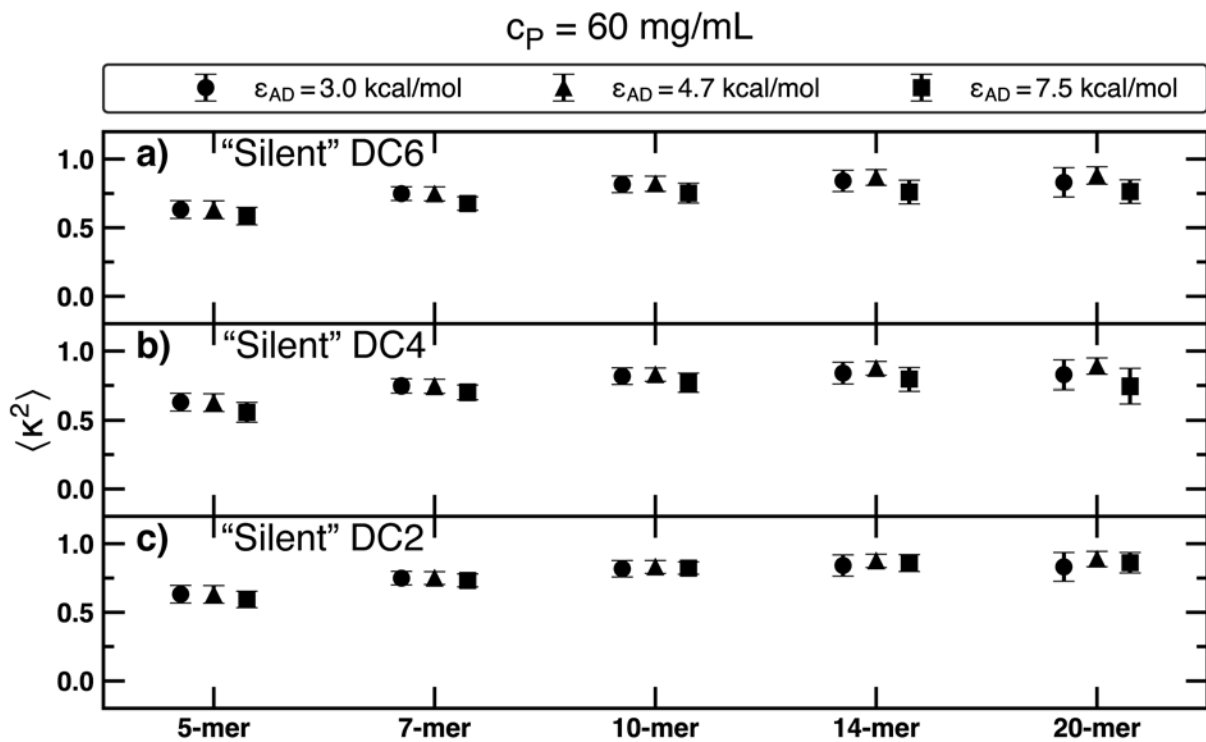


**Figure S36.** Average single chain relative shape anisotropy at  $c_P = 60 \text{ mg/mL}$  for targeted substitution of DC6 (panel a), DC4 (panel b), and DC2 (panel c). Error bars denote standard deviation over 3 replicas and 250 frames per replica.



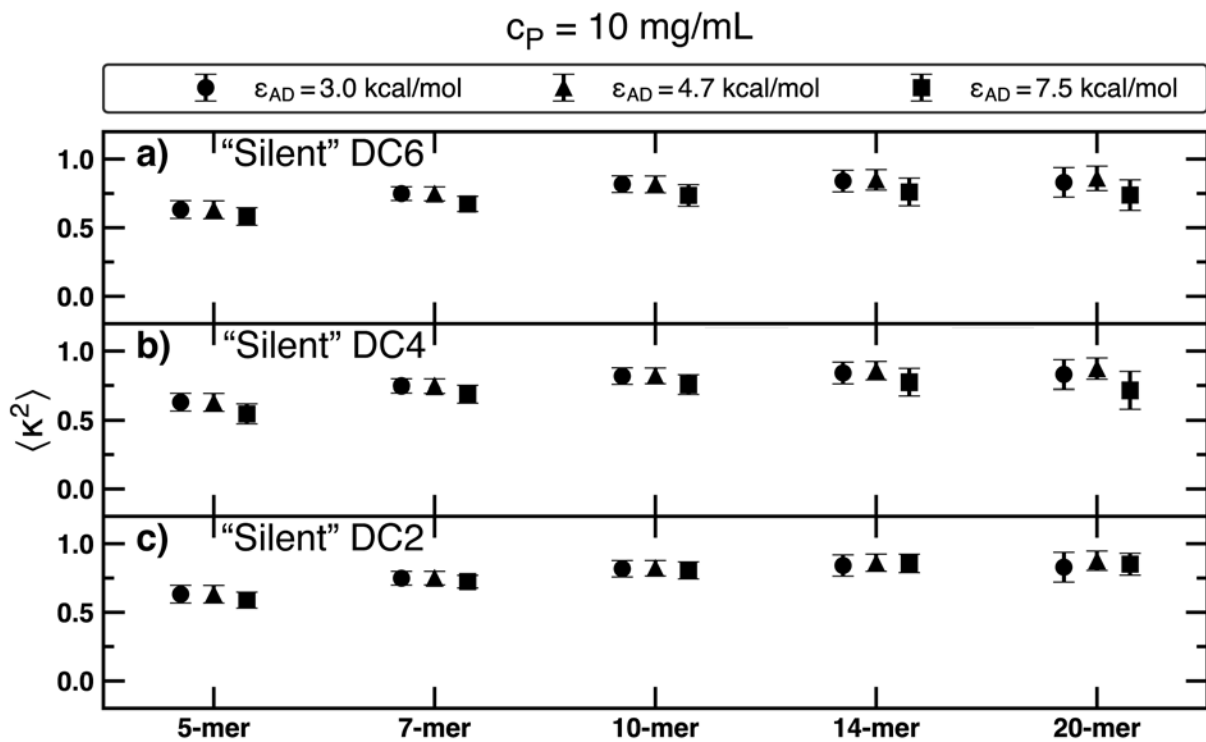


**Figure S37.** Average single chain relative shape anisotropy at  $c_P = 10 \text{ mg/mL}$  for targeted substitution of DC6 (panel a), DC4 (panel b), and DC2 (panel c). Error bars denote standard deviation over 3 replicas and 250 frames per replica.

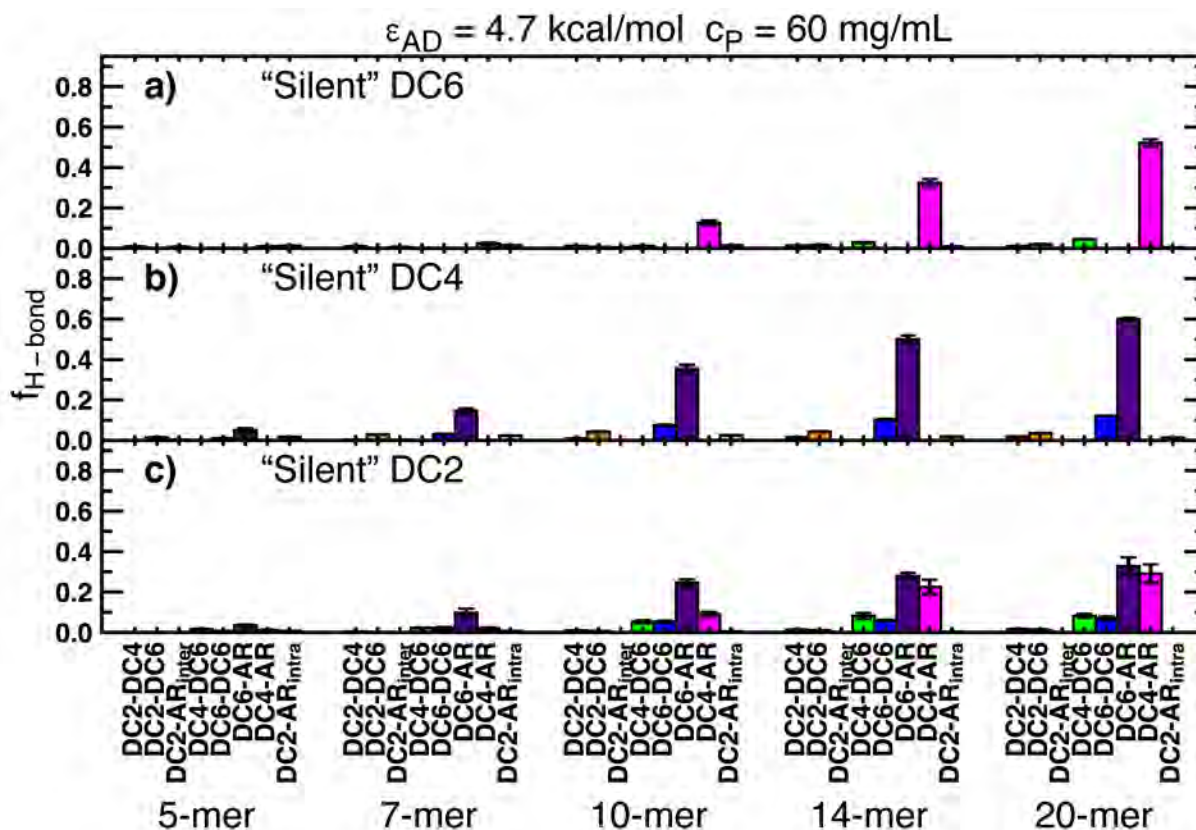


**Figure S38.** Frequency of hydrogen bonds at  $\epsilon_{AD} = 4.7 \text{ kcal/mol}$  and  $c_p = 60 \text{ mg/mL}$  for targeted substitution of DC6 (panel a), DC4 (panel b), and DC2 (panel c). Error bars denote standard deviation over 3 replicas.

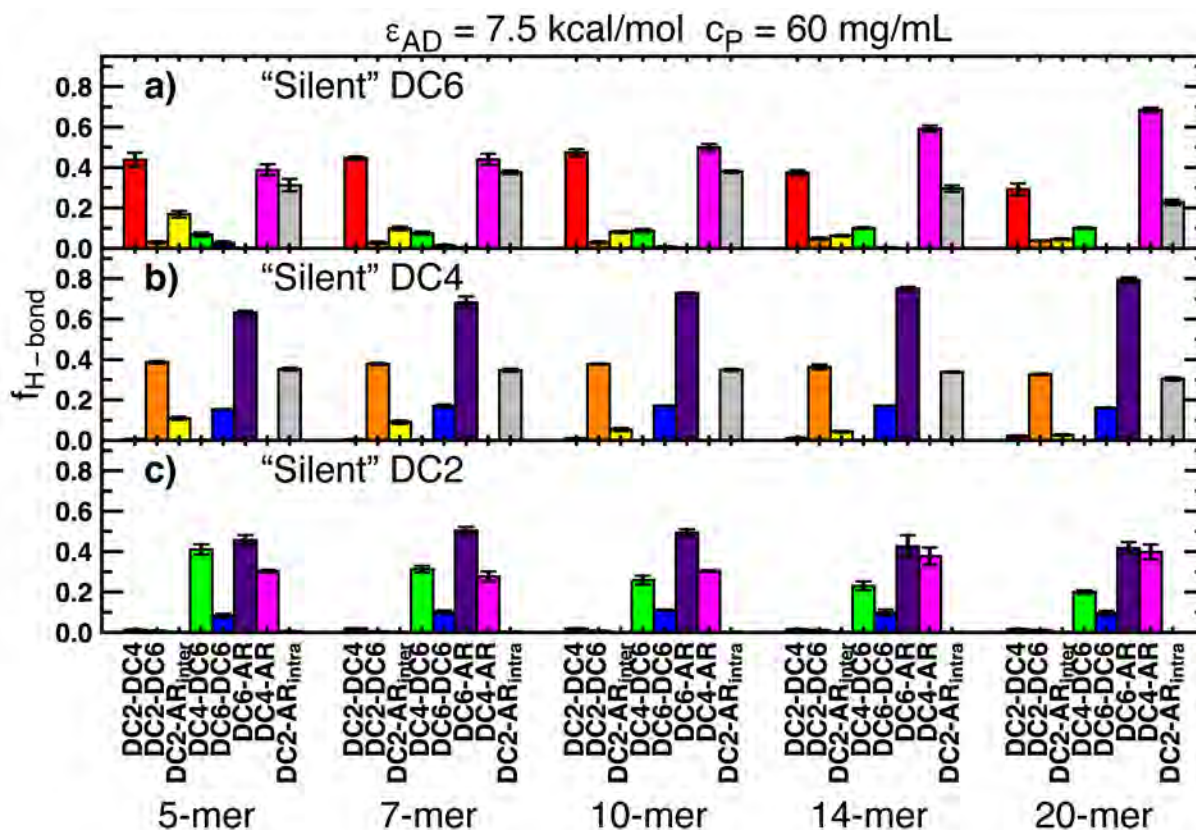


**Figure S39.** Frequency of hydrogen bonds at  $\epsilon_{AD} = 7.5 \text{ kcal/mol}$  and  $c_p = 60 \text{ mg/mL}$  for targeted substitution of DC6 (panel a), DC4 (panel b), and DC2 (panel c). Error bars denote standard deviation over 3 replicas.

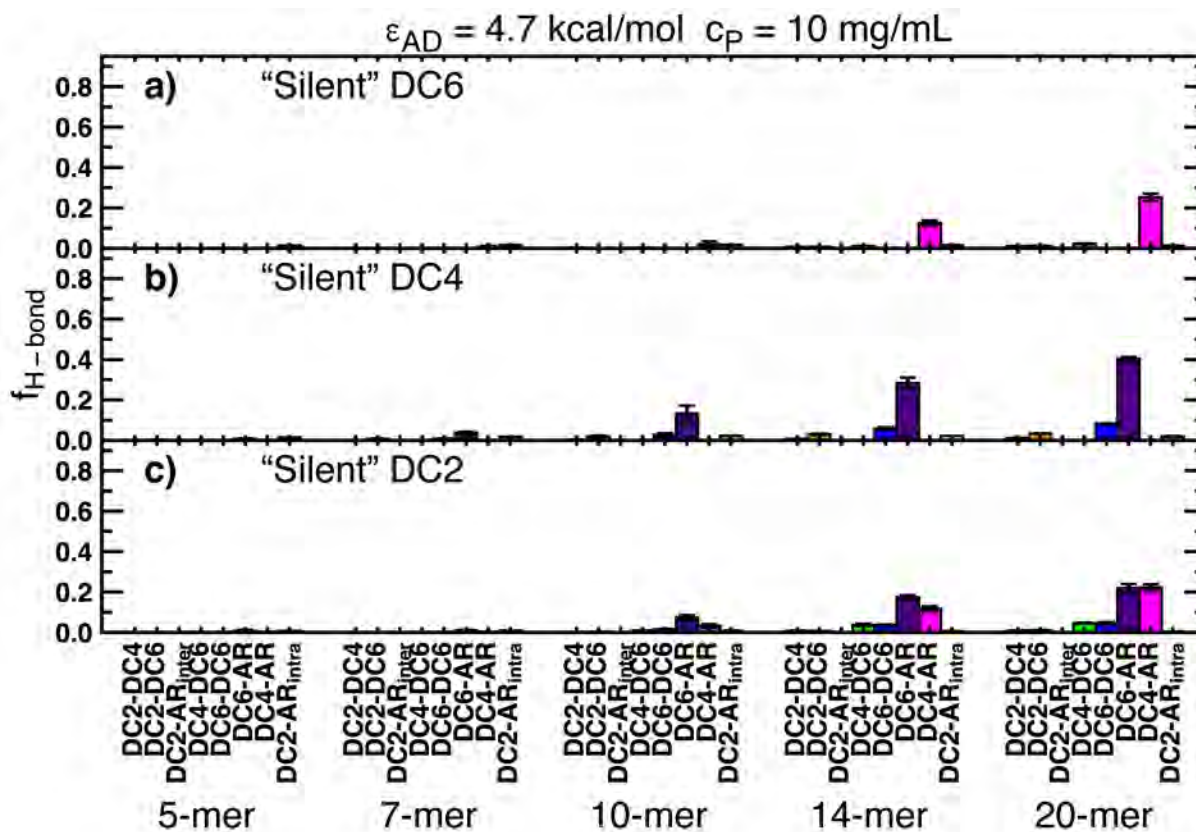


**Figure S40.** Frequency of hydrogen bonds at  $\epsilon_{AD} = 4.7 \text{ kcal/mol}$  and  $c_P = 10 \text{ mg/mL}$  for targeted substitution of DC6 (panel a), DC4 (panel b), and DC2 (panel c). Error bars denote standard deviation over 3 replicas.

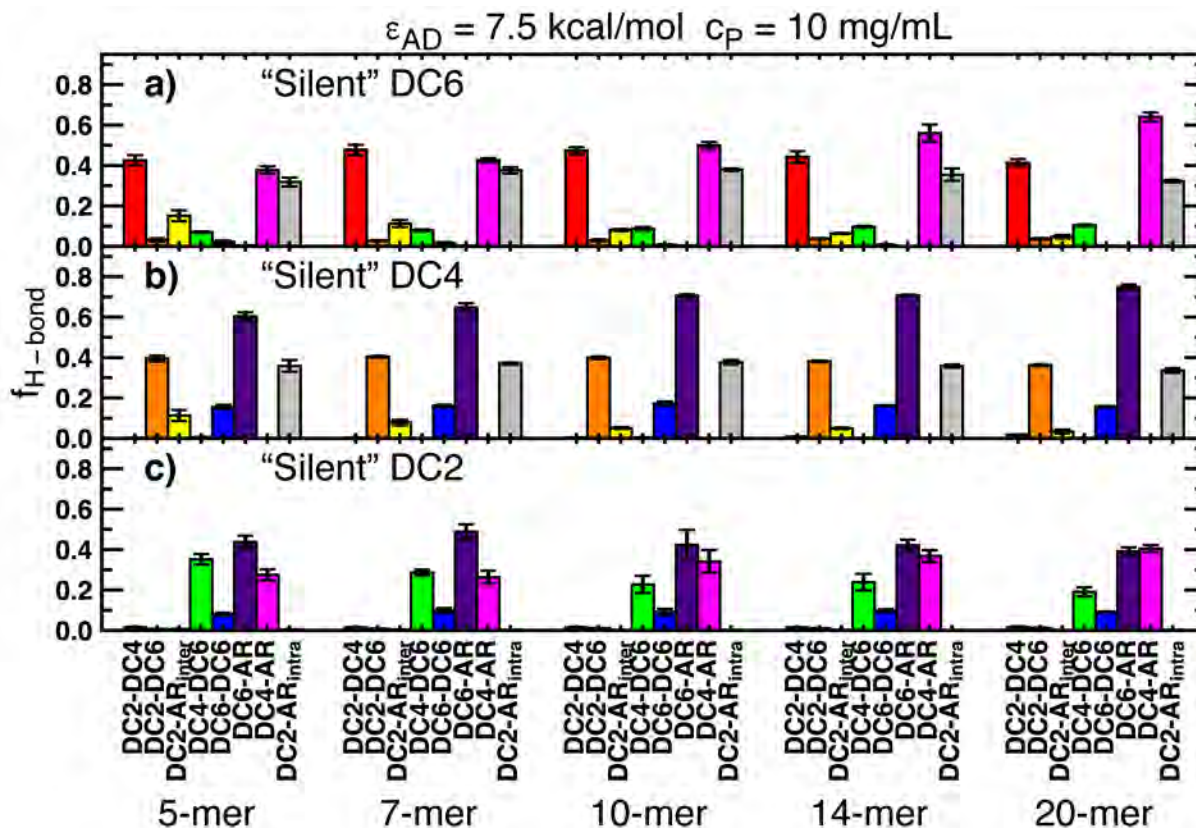


**Figure S41.** Frequency of hydrogen bonds at  $\epsilon_{AD} = 7.5 \text{ kcal/mol}$  and  $c_p = 10 \text{ mg/mL}$  for targeted substitution of DC6 (panel a), DC4 (panel b), and DC2 (panel c). Error bars denote standard deviation over 3 replicas.

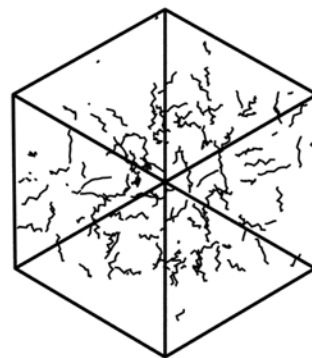
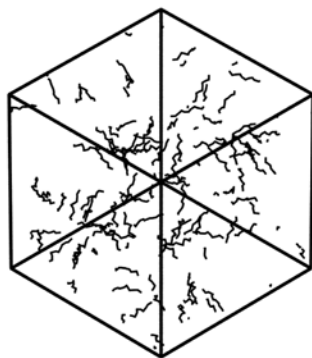
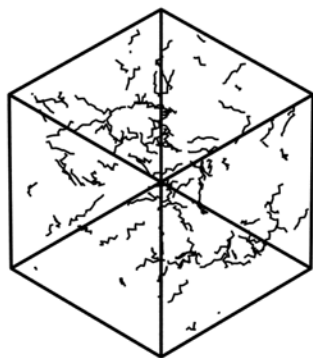
$c_p = 60 \text{ mg/mL}$ ,  $\epsilon_{AD} = 4.7 \text{ kcal/mol}$

“Silent” DC2

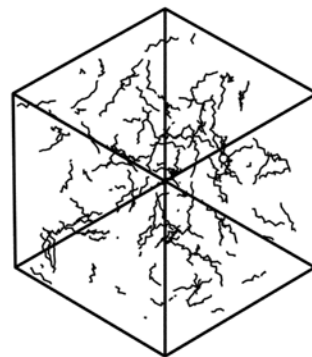
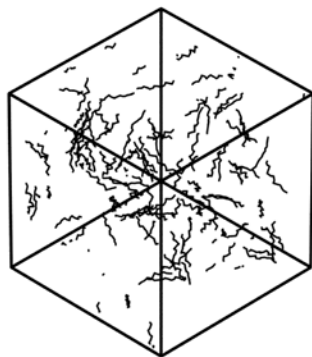
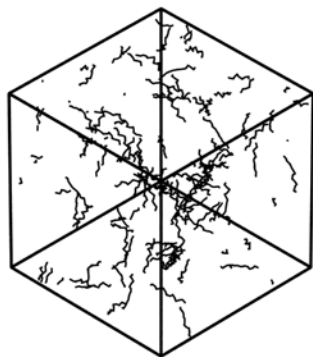
“Silent” DC4

“Silent” DC6

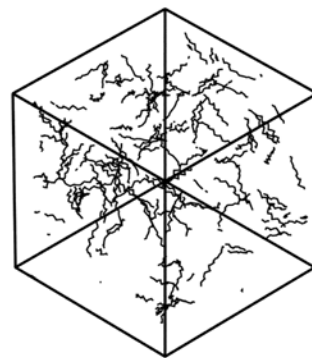
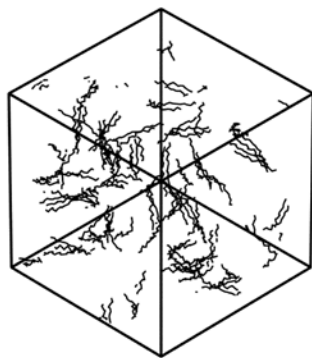
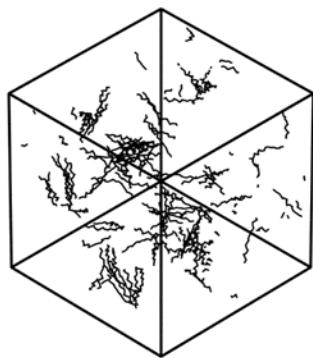
5-mer



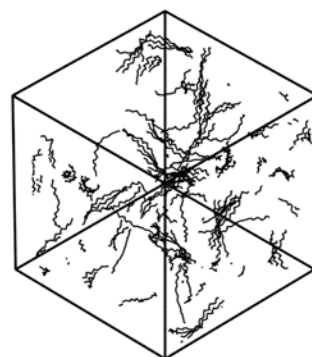
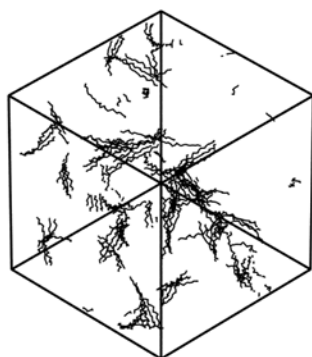
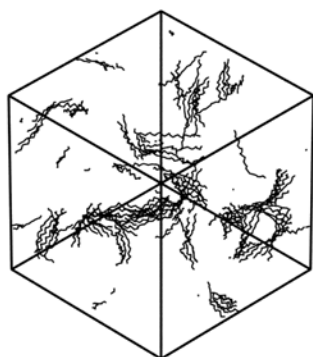
7-mer



10-mer



14-mer



20-mer

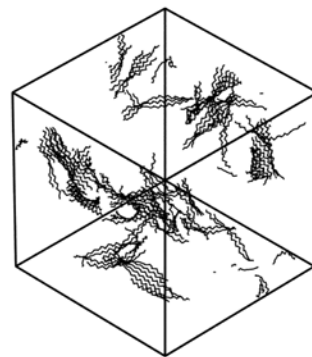
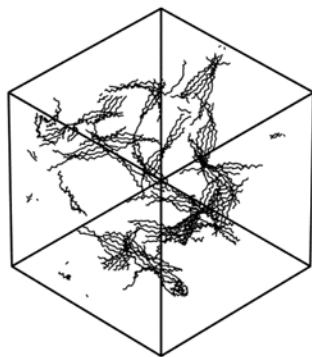
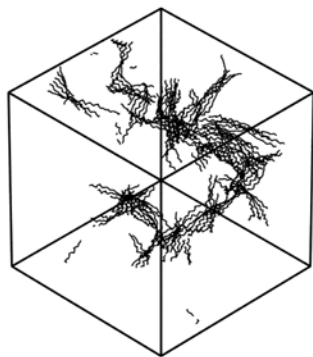


**Figure S42.** Simulation snapshots for targeted substitution of 5-mer, 7-mer, 10-mer, 14-mer, and 20-mer chains at  $c_p = 60 \text{ mg/mL}$  and  $\epsilon_{AD} = 4.7 \text{ kcal/mol}$ .

$c_p = 60 \text{ mg/mL}$ ,  $\epsilon_{AD} = 7.5 \text{ kcal/mol}$

“Silent” DC2

“Silent” DC4

“Silent” DC6

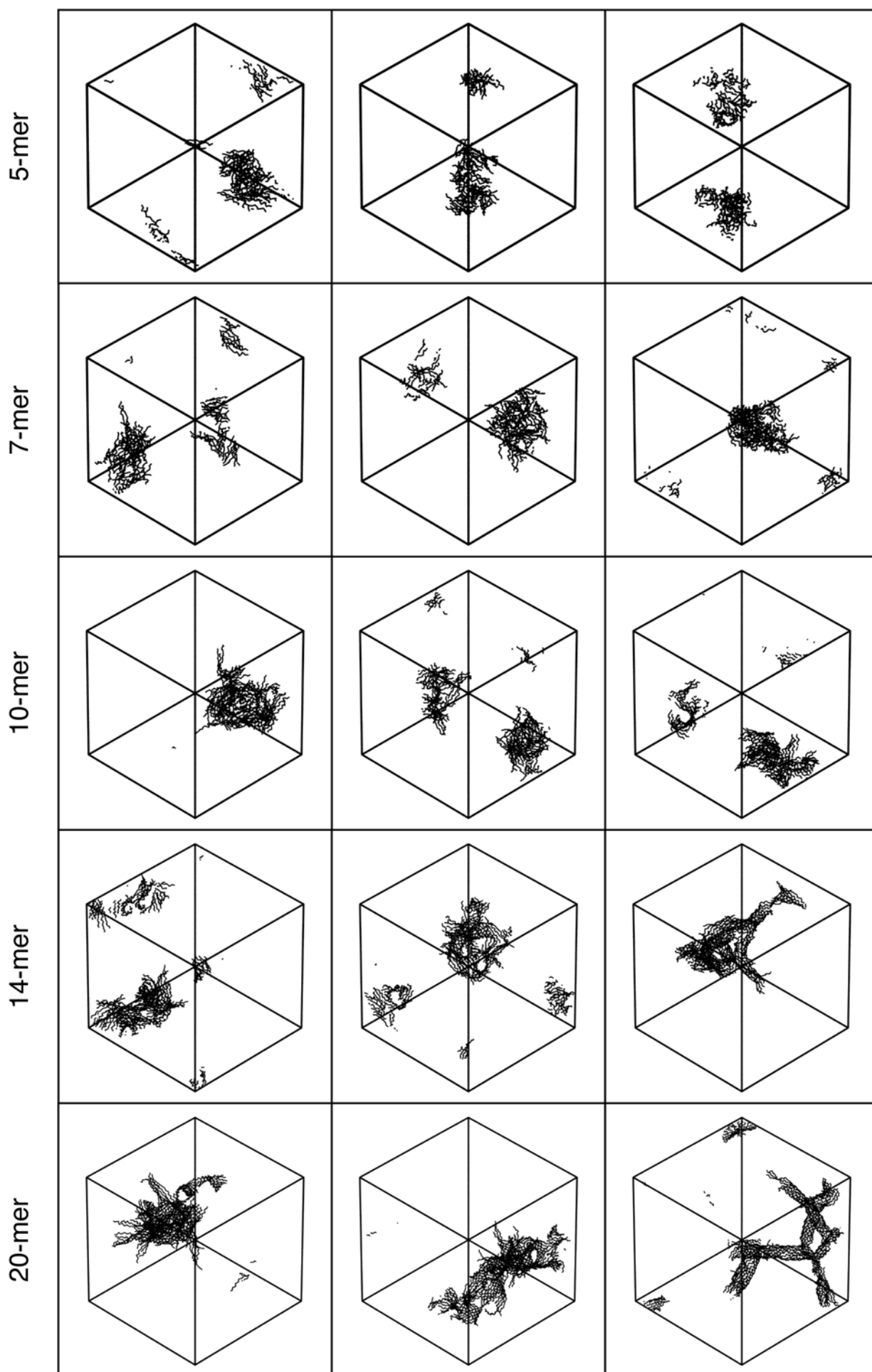


**Figure S43.** Simulation snapshots for targeted substitution of 5-mer, 7-mer, 10-mer, 14-mer, and 20-mer chains at  $c_p = 60 \text{ mg/mL}$  and  $\epsilon_{AD} = 7.5 \text{ kcal/mol}$ .

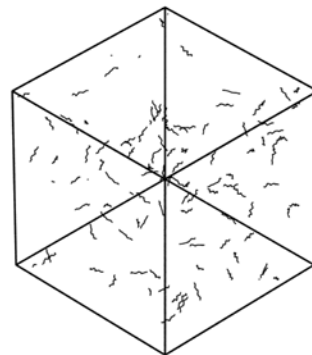
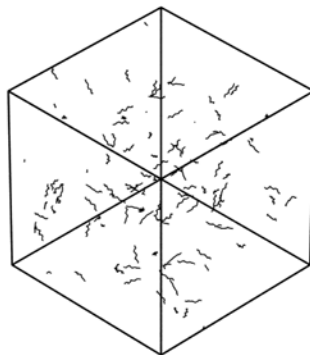
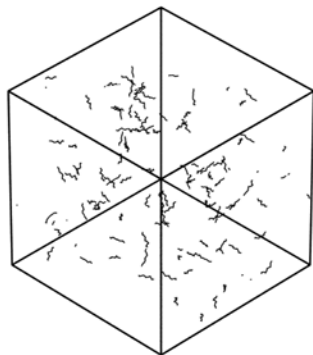
$c_p = 10 \text{ mg/mL}$ ,  $\epsilon_{AD} = 4.7 \text{ kcal/mol}$

“Silent” DC2

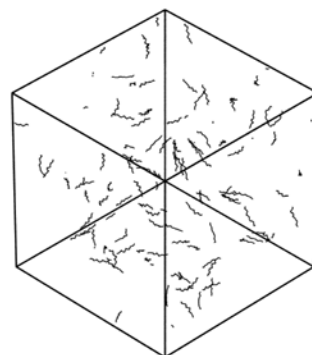
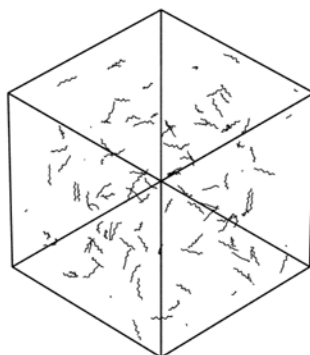
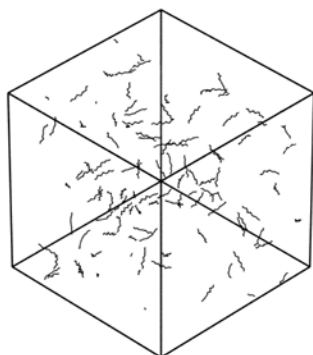
“Silent” DC4

“Silent” DC6

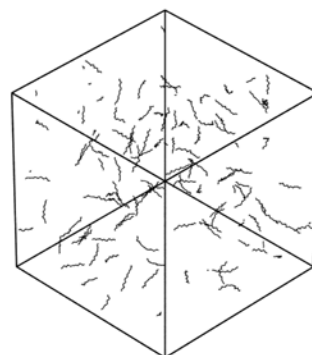
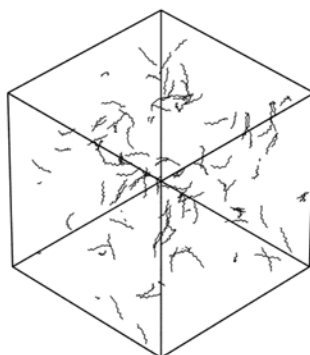
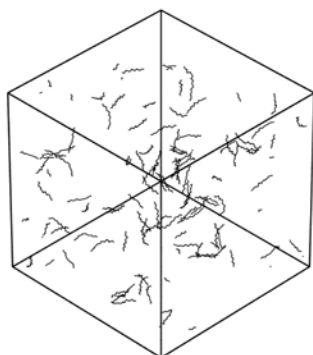
5-mer



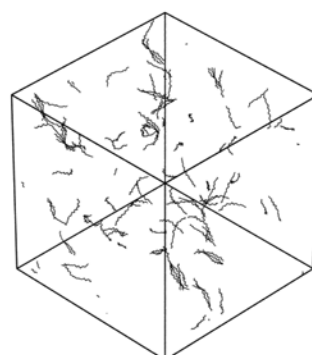
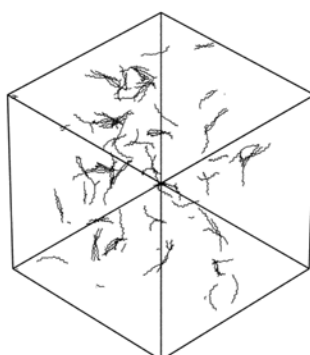
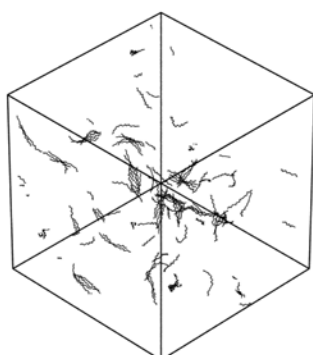
7-mer



10-mer



14-mer



20-mer

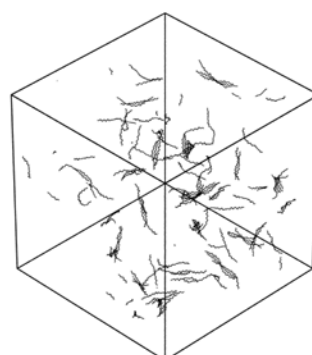
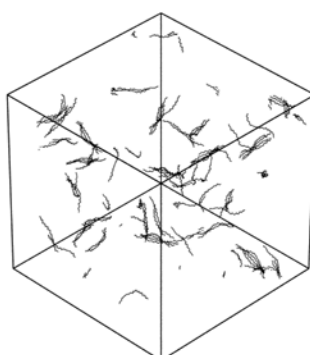
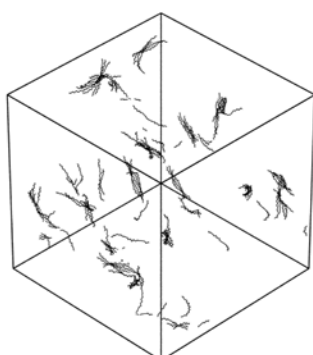


**Figure S44.** Simulation snapshots for targeted substitution of 5-mer, 7-mer, 10-mer, 14-mer, and 20-mer chains at  $c_p = 10 \text{ mg/mL}$  and  $\epsilon_{AD} = 4.7 \text{ kcal/mol}$ .



$c_p = 10 \text{ mg/mL}$ ,  $\epsilon_{AD} = 7.5 \text{ kcal/mol}$

“Silent” DC2

“Silent” DC4

“Silent” DC6

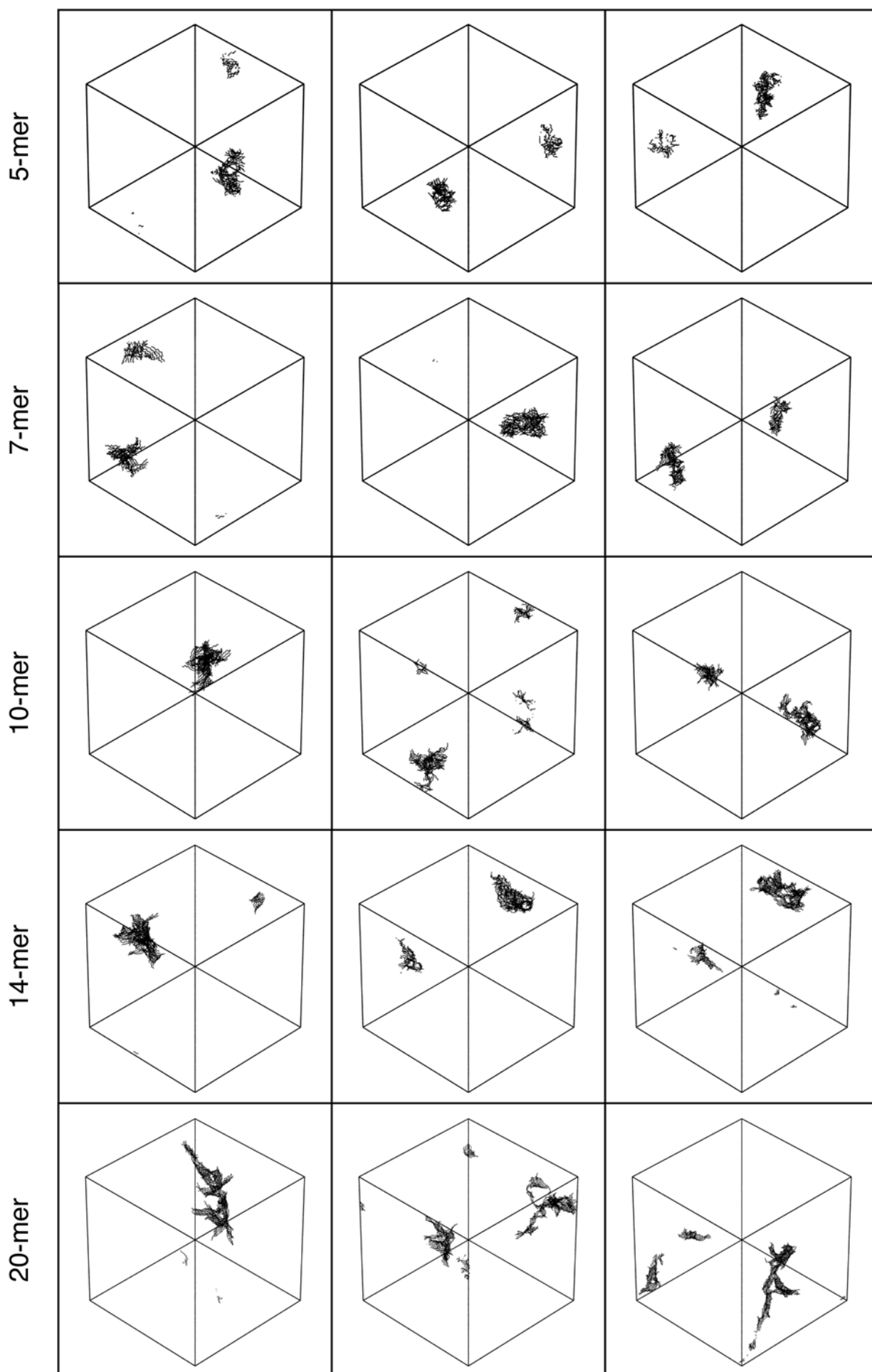


**Figure S45.** Simulation snapshots for targeted substitution of 5-mer, 7-mer, 10-mer, 14-mer, and 20-mer chains at  $c_p = 10 \text{ mg/mL}$  and  $\epsilon_{AD} = 7.5 \text{ kcal/mol}$ .

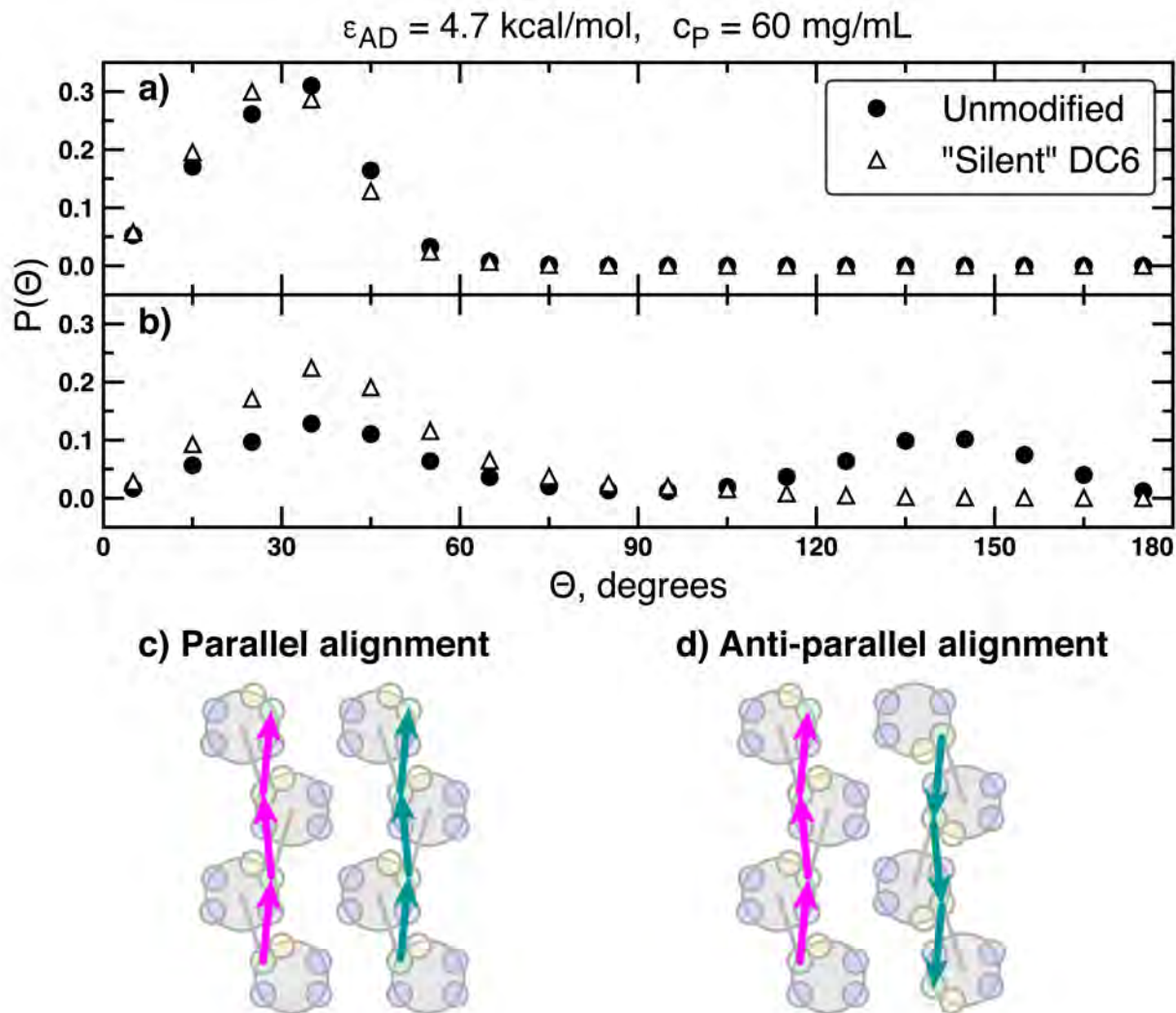


**Figure S46.** Comparison of alignment angle,  $\Theta$ , for unmodified and targeted modification of  $\alpha$ -1,3-glucan. Relative angle between monomer directors (linker-to-linker unit vector) of chains in unmodified (closed symbols), and targeted substitution of DC6 (open symbols) for intra-chain alignment (panel a) and inter-chain alignment (panel b) at  $\epsilon_{AD} = 4.7 \text{ kcal/mol}$  and  $c_P = 60 \text{ mg/mL}$ . Panels c and d show schematics of parallel and anti-parallel inter-chain alignment, respectively. Please note that monomer director vectors within one chain are not perfectly aligned, resulting in a  $\sim 30^\circ$  angle intra-chain alignment and parallel inter-chain alignment and  $\sim 150^\circ$  angle inter-chain anti-parallel alignment.

## References

1. L. M. Kroon-Batenburg, P. H. Kruiskamp, J. F. Vliegthart and J. Kroon, *The Journal of Physical Chemistry B*, 1997, **101**, 8454-8459.
2. K. Kobayashi, T. Hasegawa, R. Kusumi, S. Kimura, M. Yoshida, J. Sugiyama and M. Wada, *Carbohydrate polymers*, 2017, **177**, 341-346.